402 698

FURTHER DEVELOPMENT OF A MORE ACCURATE METHOD FOR CALCULATING BODY-WATER IMPACT PRESSURES

BY

WEN-HWA CHU

AND

DAVID R. FALCONER

TECHNICAL REPORT NO. 5
CONTRACT NO. NONR 2729(00)
SwRI PROJECT NO. 23-834-2

PREPARED FOR

BUREAU OF SHIPS
FUNDAMENTAL HYDROMECHANICS RESEARCH PROGRAM
S-R009 01 01
DAVID TAYLOR MODEL BASIN
DEPARTMENT OF THE NAVY
WASHINGTON 7, D.C.

JANUARY 1963

SOUTHWEST RESEARCH INSTITUTE
SAN ANTONIO, TEXAS

SOUTHWEST RESEARCH INSTITUTE
8500 Culebra Road, San Antonio 6, Texas

FURTHER DEVELOPMENT OF A MORE ACCURATE METHOD FOR CALCULATING BODY-WATER IMPACT PRESSURES

by

Wen-Hwa Chu
and
David R. Falconer

Technical Report No. 5
Contract No. Nonr-2729(00)
SwRI Project No. 23-834-2

Prepared for

Bureau of Ships
Fundamental Hydromechanics Research Program
Subproject S-R009 01 01
David Taylor Model Basin
Department of the Navy
Washington 7, D. C.

January 1963

APPROVED:

Herbert L. Hoffman for
H. Norman Abramson, Director
Department of Mechanical Sciences

ABSTRACT

A computer program for two-dimensional slamming of a Mariner section is discussed. The program was devised to examine the practical applicability of a previously described numerical method and to gain insight for future development of a numerical scheme should additional effort appear valuable. A discussion of this effort and the implications for the future are given.

TABLE OF CONTENTS

TABLE OF CONTENTS (Continued)

I. INTRODUCTION

A numerical method for two-dimensional water entry of a general convex body was proposed in [1] and applied in [2] to a circular cylinder. The effort in [2] shows some hope of obtaining a reasonable result if sufficiently small mesh size is employed. However, the method required further investigation because of the uncertainty in accuracy of the numerical scheme.

Because of the practical importance of ship slamming, experiments were conducted at DTMB for a Mariner section. A computer program has been written and partially debugged to aid in further development of the above-mentioned method and possible application to the Mariner section. This program, although not completely checked, yields reasonably good values of the velocity potential in comparison with analytical values for a circular cylinder at the first time step.

Based on the present knowledge, discussions are also given for future development of numerical schemes which might be worthwhile in those cases where simple fitting theories fail to yield sufficient information, or when the accuracy of experiments is in doubt.

II. FORMULATION OF THE PROBLEM

The mathematical formulation for the entry of any symmetric convex body into a two-dimensional irrotational incompressible flow field is briefly reviewed in the following:

Let the velocity potential, ϕ , in the moving coordinates x, y fixed on the body (Fig. 1) be decomposed into two parts

$$\phi = \phi' + \phi_\infty = \phi' + Vy \tag{1}$$

where

$$\phi_\infty = Vy \tag{2}$$

The perturbation velocity components u' and V', which are not necessarily small in comparison with the entry velocity V, are given by

$$\nabla\phi' = \hat{i}u' + \hat{j}v' \tag{3}$$

On the free surface the pressure is a constant, say, p_∞ , thus

$$p = p_\infty \qquad \text{(on the free surface).} \tag{4}$$

Since the free surface is rising with velocity V, the generalized Bernoulli's equation yields

$$p - p_\infty = -\rho\left[\frac{\partial\phi'}{\partial t} + \frac{1}{2}\left(v'^2 + 2v'V\right) + \frac{1}{2}u'^2 + g(y - Vt)\right] \tag{5}$$

The particles on the free surface move with the local velocity, thus if the free surface is expressed by $y - Y(x,t) = 0$ or by $x - X(y,t) = 0$ the kinematic condition is [3]

$$-\frac{\partial Y}{\partial t} - u\frac{\partial Y}{\partial x} + V = 0 \tag{6a}$$

or

$$-\frac{\partial X}{\partial t} + u - v\frac{\partial X}{\partial y} = 0 \tag{6b}$$*

where the velocity components are

$$u = u' \tag{6c}$$

$$v = v' + V \tag{6d}$$

(6b) will not be employed in this report. Also to simplify the computer program, the free surface near the contact point will not be constructed by following the particles as in [2], but will employ only equation (6a).

On the solid boundary (wetted part), the relative normal velocity is zero, hence

$$\frac{\partial \phi'}{\partial x}\cos(n,x) + \left(\frac{\partial \phi'}{\partial y} + V\right)\cos(n,y) = 0 \tag{7}$$

---

* Tangency condition of the free surface to a wedge can be shown from equation (6b) and equation (7), assuming conical flow. In general, application of this condition may be contradictory to these equations as $\frac{\partial X}{\partial t}$ may not be zero.

where n is the normal to the solid boundary. If the liquid is bounded by a finite tank, equation (7) should be applied on the tank as well as on the immerging body. If an infinite domain is considered, the disturbance vanishes at infinity, thus

$$\phi' = u' = v' = 0 \qquad \text{at very large distance from the body} \tag{8}$$

The velocity potential for irrotational incompressible flow is governed by the Laplace equation $\nabla^2\phi = 0$ and likewise

$$\nabla^2\phi' = \frac{\partial^2\phi'}{\partial x^2} + \frac{\partial^2\phi'}{\partial y^2} = 0 \tag{9}$$

III. NUMERICAL SCHEME

A. Reduction of Differential Equation

To avoid extrapolation, irregular nets are constructed with the rising free surface. In general, a six-point formula is needed for the Laplace equation. Let the five points surrounding (x, y) be $(x + h_i, y + k_i)$, $1 \le i \le 5$ (see Fig. 1). Neglecting the remainder in the Taylor's series, one finds

$$\nabla^2\phi' = \frac{1}{\Delta}\left|h_i\,,\ k_i\,,\ \phi'(x+h_i\,,\ y+k_i\,)-\phi'(x,y),\ h_i\,k_i\,,\ \tfrac{1}{2}\,k_i^2\right|$$

$$+\frac{1}{\Delta}\left|h_i\,,\ k_i\,,\ \tfrac{1}{2}\,h_i^2\,,\ h_i\,k_i\,,\ \phi'(x+h_i\,,\ y+k_i\,)-\phi'(x,\,y)\right| = 0 \qquad (10a)$$

where the points should be selected so that

$$\Delta = \left|h_i\,,\ k_i\,,\ \tfrac{1}{2}\,h_i^2\,,\ h_i\,k_i\,,\ \tfrac{1}{2}\,k_i^2\right| \neq 0 \qquad (10b)$$

In general, the error is about the first order of the maximum of h_i and k_i. If equal arm rectangular nets could be used, the local truncation error would be second order.

When the net through the center point 0 consists of two perpendicular lines ($h_2 = h_4 = k_1 = k_3 = 0$), equation (10) reduces to the five-point formulas [4]

$$\frac{2}{h_1+h_3}\left[\frac{\phi_1'-\phi_0'}{h_1}+\frac{\phi_3'-\phi_0'}{h_3}\right]+\frac{2}{k_2+k_4}\left[\frac{\phi_2'-\phi_0'}{k_2}+\frac{\phi_4'-\phi_0'}{k_4}\right]=0 \qquad (11a)$$

---

* $|a_i\,,\ b_i\,\cdots|$ is a determinant, the i'th row of which is given.

where $\phi_i' = \phi'(x+h_i, y+k_i)$, $\phi_o' = \phi'(x, y)$

In the square net domain, $h_1 = h_3 = k_2 = k_4$, it further reduces to

$$\phi_1' + \phi_2' + \phi_3' + \phi_4' - 4\phi_o' = 0 \tag{11b}$$

This will be employed for the domain bounded by the initial free surface, the line of symmetry and the lines $x = L$, $y = -L$.

B. Difference Form for the Boundary Conditions

In general, the first derivatives can be expressed by a three-point formula

$$\frac{\partial \phi'}{\partial x} \cong \frac{1}{|h_i, k_i|} \left| \phi'(x+h_i, y+k_i) - \phi'(x, y), k_i \right| \tag{12a}$$

$$\frac{\partial \phi'}{\partial y} \cong \frac{1}{|h_i k_i|} \left| h_i, \phi'(x+h_i, y+k_i) - \phi'(x, y) \right| \tag{12b}$$

in which the point x, y is on the boundary while the neighboring points are taken so that $|h_i, k_i| \neq 0$. The error would be first order in h_i and k_i. When $h_1 = 0$, $k_1 = k_2$, equations (12a, b) reduce to

$$\frac{\partial \phi'}{\partial x} \cong \frac{\phi_2' - \phi_i'}{h_2} \tag{13a}$$

$$\frac{\partial \phi'}{\partial y} \cong \frac{\phi_i' - \phi_o'}{k_1} \tag{13b}$$

The boundary condition equation (7) is then approximated by

$$\frac{\phi_2' - \phi_1'}{h_2} \cos(n,x) + \frac{\phi_1' - \phi_0'}{k_1} \cos(n,y) \cong -V \cos(n,y) \tag{14}$$

At the keel

$$\phi_1' - \phi_0' = -V k_1 = Vh \tag{15}$$

By symmetry $\phi_1' = \phi_3'$ across the line of symmetry, equation (11b) is reduced to

$$2\phi_1' + \phi_2' + \phi_4' - 4\phi_0' = 0 \tag{16}$$

For the point directly under the keel, $\phi_2' - \phi_0' = -Vh$, h is the size of the square net in the inner domain. Equation (16) reduces to

$$2\phi_1' + \phi_4' - 3\phi_0' - Vh = 0 \tag{17}$$

Equation (10a) can be represented by

$$A_1\phi_1' + A_2\phi_2' + A_3\phi_3' + A_4\phi_4' + A_5\phi_5' - A_0\phi_0' = 0 \tag{18}$$

where $A_0 > 0$.

For other net points directly under the body, equation (14) can be used to eliminate the boundary point, say i = 2. One finds, making

$$\phi_1' \to \phi_0',\ \phi_2' \to \phi_1',\ \phi_0' \to \phi_2,\ k_1 \to -k_2,\ h_2 \to h_1$$

in equation (14) before substituting into equation (18),

$$A_1\phi_1' + A_2\left[\phi_0' - (\phi_1' - \phi_0')\frac{k_2\cos(n,x)}{h_1\cos(n,y)} - Vk_2\right] + A_3\phi_3' + A_4\phi_4' + A_5\phi_5' - A_0\phi_0' = 0$$

or

$$\left[A_1 - \frac{A_2 k_2}{h_1}\cdot\frac{\cos(n,x)}{\cos(n,y)}\right]\phi_1' + A_3\phi_3' + A_4\phi_4' + A_5\phi_5' - \left(A_0 - A_2 - A_2\frac{k_2\cos(n,x)}{h_1\cos(n,y)}\right)\phi_0' - A_2 Vk_2 = 0 \tag{19}$$

It is noted that for convex bodies, $\frac{\cos(n,x)}{\cos(n,y)} \leq 0$

The infinite domain is approximated by a sufficiently large finite domain, thus the boundary conditions at the large distance $x = L$ and $y = -L$ are simply

$$\phi' = 0 \qquad \text{at } x = L \text{ or } y = -L \tag{20}$$

Finally, the kinematic and dynamic boundary conditions of the free surface must be imposed. Unfortunately the spray at the contact point cannot be traced due to the presence of a singularity, at least in the present scheme [2], hence as in the analytic studies of pile-up water effect, the particle at the new contact point comes from a neighboring point on the free surface. Using an explicit scheme, the new free surface is constructed by the difference approximation to equation (6a)

$$Y(x, t+\delta t) = Y(x,t) + \left[v - u\,\frac{Y(x+h,t) - Y(x-h,t)}{2h}\right]\delta t \tag{21}$$

The truncation error of equation (21) is first order in δt but second order in $\Delta X = h$.

The dynamic condition on the free surface and the Bernoulli's equation yields

$$\frac{\partial \phi'}{\partial t} = -\left[\frac{1}{2}(v'^2 + 2v'V) + \frac{1}{2}u'^2 + g(y - Vt)\right] \tag{22}$$

Correct to first order in δt, the potential on the free surface is given by

$$\phi'(x, Y(x, t+\delta t), t+\delta t) \cong \phi'(x, Y(x,t), t) + \frac{\partial \phi'}{\partial t}\delta t + \frac{\partial \phi'}{\partial y}\frac{\partial Y}{\partial t}\delta t$$

$$\cong \phi'(x, Y(x,t), t) + \left(\frac{1}{2}v'^2 - \frac{1}{2}u'^2\right)\delta t - v'u'\frac{\partial Y}{\partial x}\delta t - g\left[Y(x,t) - \int_0^t V\,dt\right] \tag{23}$$

where

$$\frac{\partial Y}{\partial x} \cong \frac{Y(x+h,t) - Y(x-h,t)}{2h} \quad \text{if } Y(x-h,t) \text{ exists} \tag{24a}$$

$$\frac{\partial Y}{\partial x} \cong \frac{Y(x+h,t) - Y(x,t)}{h} \quad \text{otherwise} \tag{24b}$$

$$u' \cong \frac{\phi'(x+h,t) - \phi'(x-h,t)}{2h} \tag{24c}$$

$$v' \cong \frac{\phi'(x, Y(x, t+\delta t)) - \phi'(x, Y(x,t))}{Y(x, t+\delta t) - Y(x,t)} \tag{24d}$$

C. Graded Nets

To reduce the number of points, graded nets [5] are employed in the domain below the free surface. Diagonal cross nets are used when making the transition to a coarser subregion. Equation (11b) is applicable at the center of the cross net by taking the four corner points of the cross as neighboring points.

D. Successive Over-Relaxation Procedure

The successive over-relaxation procedure and its sufficient conditions for convergence are given in [6], [7], [8], and elsewhere. It seems that if one cannot prove the largest eigen values of the iteration matrix are less than one for convergence (or greater than one for divergence), the convergence of the process at each time step is best determined by carrying out the process on the computer. Let the difference equation take the form

$$c_1 \phi_1' + c_2 \phi_2' + c_3 \phi_3' + c_4 \phi_4' + c_5 \phi_5' + c_6 - c_0 \phi_0' = R \tag{25}$$

where the residue, R = 0 for the exact solution of the difference scheme. The over-relaxation procedure is to adjust ϕ_0' to $\bar{\phi}_0'$ such that the residue R becomes $(1-\omega)R$, ω being the over-relaxation factor, i.e.

$$\bar{\phi}_0' = \frac{\omega}{c_0} \left[c_1 \phi_1' + c_2 \phi_2' + c_3 \phi_3' + c_4 \phi_4' + c_5 \phi_5' + c_6 \right] + (1-\omega) \phi_0' \tag{26}$$

where $1 \leq \omega < 2$

This process is applied successively and repeatedly until all ϕ_*' converge by the criterion that

$$\left| \bar{\phi}_*' - \phi_*' \right| < \delta \tag{27}$$

The appropriate value of δ is best selected empirically, such as by comparing the results for δ and $\frac{\delta}{10}$.

E. Time Step and Space Mesh Sizes

As mentioned, the contact point is a singular point, the particle at the contact point is lost in an infinitesimally thin spray. Since the new effective contact point comes from a neighboring point, it seems that the additional effect of the body is best taken into account by taking a time step so that one of the neighboring points becomes the next contact point. For this reason, the value of the time step cannot be set arbitrarily. Admitting the presence of a singularity at the contact point, one must impose a relatively stringent space mesh size so that the magnitude of error in $\frac{\partial \phi'}{\partial t}$, and thus the pressure p, is admissible. Because the space mesh size is limited by the capacity of the computer, one must therefore set an approximate value of δt or a lower bound to the value of δt in the program. This, however, does not insure that the truncation error in time would be sufficiently small.

To insure a good approximation in the present formulation (except possibly in the infected region near the singular contact point), one must show that the apparent truncation error is negligible by changing mesh sizes both spacewise and timewise.

IV. ANALYTIC SOLUTION FOR THE FIRST TIME STEP, t_1

In the present numerical scheme, the effect of the body is not felt before the first time step. Therefore, the free surface is flat and the velocity potential ϕ' remains zero on the free surface. Therefore, the analytic solution for a reflected body and fluid domain can be used as a limiting value to check the computer program and its accuracy. For simplicity, the circular cylinder will be employed for checking purposes. The known analytic solution for flow normal to obstacles bounded by two circular arcs [9] is given below:

Let all lengths be nondimensionalized by the semi-wetted width. In the complex z plane (Fig. 2),

$$z = \underline{x} + i\underline{y} = \cot t = \frac{i\left(e^{it} + e^{-it}\right)}{e^{it} - e^{-it}} \tag{28}$$

The complex potential, W is given by:

$$W = \phi + i\psi = n \csc(nt) = \frac{2ni}{e^{int} - e^{-int}} \tag{29}$$

From equation (28) $e^{it} = \sqrt{\frac{z+i}{z-i}}$, thus

$$W = \frac{2ni}{\left(\frac{z+i}{z-i}\right)^{\frac{n}{2}} - \left(\frac{z+i}{z-i}\right)^{-\frac{n}{2}}} = \frac{2ni}{\left(\frac{r_2}{r_1}\right)^{\frac{n}{2}} e^{i\frac{n}{2}(\sigma_2 - \sigma_1)} - \left(\frac{r_1}{r_2}\right)^{\frac{n}{2}} e^{-i\frac{n}{2}(\sigma_2 - \sigma_1)}} \tag{30}$$

On the circular arc (-$\underline{x}$ side), $\sigma_2 - \sigma_1 = -\frac{\pi}{n}$, n being implicitly defined by the semi-thickness of the section which is $\cot\left(\frac{\pi}{2n}\right)$. Therefore,

$$\psi = 0 \qquad \text{(streamline)} \tag{31a}$$

$$\phi = \frac{-2n}{\left(\frac{r_2}{r_1}\right)^{\frac{n}{2}} + \left(\frac{r_1}{r_2}\right)^{\frac{n}{2}}} \tag{31b}$$

It is clear that the coordinate system is fixed on the body.

At infinity, for t = 0

$$\frac{dW}{dz} = \underline{u} + i\underline{v} = \frac{n^2 \csc(nt)\cot(nt)}{\csc^2 t} \longrightarrow 1 \tag{32a}$$

i.e. $V = \underline{u}_\infty = 1$, $\underline{V}_\infty = 0$

Therefore, the velocity at infinity is also normalized to unity. On the free surface, $\sigma_2 = \sigma_1 = \pi$ or $\sigma_2 = \sigma_1 = 0$, therefore

$$\phi = 0 \tag{32b}$$

In the present numerical scheme $\phi' = 0$ at the first time step on the free surface, $\underline{x} = 0$, thus

$$\phi' = \phi - \underline{u}_\infty \underline{x} = \phi - V(y - y_r) \tag{33}$$

$$\underline{x} \longrightarrow y - y_r \ , \ \underline{y} \longrightarrow x \tag{33a}$$

$$r_2 = \sqrt{\underline{x}^2 + (\underline{y}-1)^2} = \sqrt{(y_T - y)^2 + (1-x)^2} \tag{33b}$$

$$r_1 = \sqrt{\underline{x}^2 + (\underline{y}+1)^2} = \sqrt{(y_T - y)^2 + (1-x)^2} \tag{33c}$$

By coincidence the values of ϕ' obtained on a desk calculator agreed excellently with the values of ϕ on the boundary in [2]. This fact is discovered from computer results (Fig. 3) based on much more stringent convergent criteria in the present computer program. The limiting value of ϕ' on the cylinder at the first time step is governed by both equation (31b) and equation (33) in terms of entry velocity, V times semi-wetted width, b.

V. COMPARISON OF NUMERICAL AND ANALYTIC SOLUTION AT t_1

The water entry of a circular cylinder at time t_1 possesses a simple analytic solution equivalent to the limiting case of infinite domain and infinitesimal mesh sizes in the present numerical formulation.

This yields some guidance as to the size of the meshes, size of the domain and the magnitude of the convergence factor.

The same example as in [2] and [10] is used. A domain of 10" x 10" is taken when the semi-wetted width is 1" to simulate an infinite fluid domain. The present computer program grades the net three times. The inner domain in this example is 2-1/2" x 2-1/2" covered by 1/8" x 1/8" square meshes as in [2].

At first, a convergence factor of $\delta = 10^{-3}$ was used which is very close to the convergence criterion used for the desk calculator results reported in [2]. The latter criterion makes all the residues lie between + .002 and −.001, when the diagonal coefficient is normalized to 4 and the value of ϕ' is cut off at 10^{-3}. Successive over-relaxation with $\omega = 1$, yields considerably lower values of ϕ' on the body than those reported in [2].

Next, over-relaxation results with $\delta = 10^{-4}$ and $\delta = 10^{-5}$ and $\omega = 1.25$ are obtained for the same domain and shown in Figure 3. It

shows convergence with respect to δ and the large probable error if a large δ such as 10^{-3} were used. Hence, $\delta = 10^{-4}$ or smaller should be assigned.

It is interesting to note that a large value of ω ($\omega = 1.9$ estimated on the basis of a uniform square net) was also tried on the 10" x 10" domain with $\delta = 10^{-5}$. It was hoped that a faster rate of convergence of the over-relaxation procedure [6] could be achieved; however, the process diverged. This is due to the fact that, while all other sufficient conditions for convergence are satisfied, the graded net used does not satisfy property "A" [7]. This may be shown by contradiction. No additional values of ω have been tried. Based on experience, it is quite likely $\omega = 1.25$ can be used at all times. If the process tends to diverge after a few cycles, the value of ω can be replaced by unity for further calculations.

An almost completed result for a 20" x 20" domain with $\delta = 10^{-5}$, $\omega = 1.25$ shows practically the same value of ϕ' (to almost 4 figures) at the keel. The computation was not completed to conserve machine time, but residues spot-checked were already less than 3×10^{-5}. Thus, a 10" x 10" domain should be adequate, unless higher accuracy is desired.

Analytic values of ϕ' (Fig. 3) from equations (31b) and (33) are in good agreement with the converged numerical results. Remaining differences are mainly due to the mesh size of the inner domain. One

may conclude that for spacewise convergence, the inner domain should have a fine mesh size of at least 1/8 of the semi-wetted width at the first time step. For better accuracy, smaller mesh size is needed.

The process, however, must converge both spacewise and time-wise. An error of 0.001 ft^2/sec in $\Delta\phi$ across a $\delta t = .0004$ sec. in a medium (water) of $\rho = 1.938$ $slug/ft^3$ results in an absolute error E_p in pressure

$$E_p = 1.938 \ slug/ft^3 \times \frac{.001 \ ft^2/sec}{.0004 \ sec} = 48.4 \ \#/ft^2$$

The maximum pressure at initial time of contact from compressible theory [11] for an entry velocity of 1 ft/sec is

$$p_o = \rho c V = 1.938 \ slug/ft^3 \times 4794 \ ft/sec \times 1 \ ft/sec = 9,291 \ \#/ft^2 \quad (34)$$

In this example, V = 8.5 ft/sec, $p_o = 78,970$ $\#/ft^2$. Although the pressure drops rapidly, it is very likely that the maximum pressure would be around a few thousand $\#/ft^2$ at the time of interest, at which time the incompressible theory might be applicable, thus an error in ϕ' of 10^{-3} ft^2/sec appears acceptable. It is clear that larger error in ϕ' exists in the vicinity of the contact point.

For sufficiently small δt, error in pressure would be proportional to $\frac{\Delta x}{V \Delta t}$. Assuming that the result based on the case where $\delta t = .0003227$, $(\Delta x)_{\text{inner domain}} = 1/8"$ and V = 8.5 ft/sec in [2]

is reasonable, then it would be desirable to make

$$\frac{\Delta x}{V\,\delta t} < \frac{\frac{1}{8} \times \frac{1}{12}\ ft}{8.5\ ft/sec \times .0003227\ sec} = 3.798 \tag{35a}$$

or

$$\frac{V\,\Delta t}{\Delta x} > \frac{8.5 \times .0003227}{\frac{1}{96}} = 0.2633 \tag{35b}$$

One must be cautioned that this criterion is not reliably established, analytically or empirically.

VI. APPLICATION TO MARINER SECTION

The planning for the application of the present method to a Mariner section will be presented. In view of the substantial funding which would be required and uncertainty in the reliability of the numerical procedure, the program has not been actually carried out.

A. Description of Mariner Section

The offsets of the Mariner model (1/20) were given by DTMB and shown in Table I. The shape of the Mariner model and pressure gauge locations are given in Figure 4. For estimation of δt and the size of the domain L, the time of contact of the pressure gauge with the water, the duration of interest and the maximum wetted width b_{mx} corresponding to the depth of submergence y_{mx} are shown in Table II. These values are quite approximate, since the effect of spray and/or pile up of water is not included.

B. Size of Fluid Domain

The number of net points would be proportional to the square of the dimension of the domain, if uniform mesh size were used. Some reduction in this number is achieved by graded nets. The present program will double the inner domain mesh size twice while grading the domain twice. To approximate the infinite domain, the size of the domain in the numerical method should be about ten times the outboard location of the pressure gauge concerned, or larger. If good accuracy

is sought at times near the end of the pressure record, a much larger domain would be required. The memory capacity of the computer (IBM 7090) limits the number of net points to about 20,000. Since the maximum pressure on the ship bottom moves outboard during slamming and the maximum value at the keel (at instant of contact) requires a compressible theory, the planning takes into account prediction of pressure at the gauge 2-1/4" outboard, as well as the gauge at the keel. For these reasons, the size of the domain L would be about 25".

C. Time Interval

It seems that the larger the number of steps taken before the time of interest, the better the nonlinear effect would be included. To reduce the machine time, three steps before time of contact of the pressure gauge (2-1/4" outboard) is assigned arbitrarily as a compromise and five steps after time of contact will yield four values of pressure at the fourth to the seventh step. Therefore, a minimum of eight steps is needed. The case of $V = 5.67$ ft/sec will be selected. δt thus should be around .00147/3 sec = .00049 sec. Since δt cannot be arbitrarily assigned in the present scheme, but would be in the neighborhood of the assigned δt, this value will be set as 0.00040 sec for the case in consideration.

D. Space Mesh Size

Assume that $\frac{\Delta x}{V \Delta t}$ for the inner domain should be less than the value given by equation (35a). If V = 5.67 ft/sec, t = .00040 sec, then Δx = 3.80 x 5.67 x .00040 x 12" = .1034". Likewise, if V = 5.67 ft/sec t = .00049 sec, then Δx = 3.80 x 5.67 x .00049 x 12" = .1267".

Therefore, it seems that one should take Δx = 1/8" or preferably 1/16" or both. Since b ≥ 1.20", $\frac{\Delta x}{b} < \frac{1}{8 \times 1.2} < \frac{1}{8}$, which also seems to be a reasonable choice based on results for the circular cylinder.

E. Approximate Number of Net Points

Case (a) $(\Delta x)_{\text{inner domain}}$ = 1/8"

The size of the inner domain is taken to be slightly larger than twice the gauge location, or 2 x 2.5" = 5". Use graded nets composed of 1/8" mesh size outward to 5" then 1/4" mesh size to 15", 1/2" to 25"; similarly downward. This requires 6,400 net points plus about 800 added net points, which includes the points added in the irregular domain up to 8 steps.

Case (b) $(\Delta x)_{\text{inner domain}}$ = 1/16"

Similarly, graded nets are composed of 1/16" mesh size to 5", 1/8" to 15" and 1/4" outward to 25". This requires 19,600 net points plus about 1,440 added net points totaling 21,040. If necessary, slight adjustment could be made to suit the memory capacity of the computer (IBM 7090).

F. Cost Estimate

As an approximate minimum cost estimate, the time required for convergence of the over-relaxation procedure is assumed to be directly proportional to the number of net points; use is then made of the information gained from the "checkout" results for a circular cylinder. Based on an IBM 7090 renting for $ 500 an hour, 7,200 net points and 8 steps would require $ 600 x 8 or $ 4,800, provided the computer program had been completely checked out. The case of 21,040 net points would require $ 1,800 x 8 or $ 14,400. It would be preferable to have both cases, as a comparison would indicate the magnitude of truncation error present.

It is concluded that the cost is much higher than the funds available and the application of the present method to the Mariner section will not be carried out.

VII. COMPUTER PROGRAM

A. General Description

A computer program based on the theory previously presented has been written and partially debugged. The program was written in the FORTRAN language to be run on the IBM 7090. A description of the program and accompanying general flow diagram will be presented in this section. A more detailed description and flow diagram is found in the appendix.

Essentially, the problem may be thought of as a successive over-relaxation problem. The general scheme of the program is to first initialize all of the mesh points; then a calculation is made to advance from the initial time, $t_0 = 0$, to what will be referred to as t_1. At t_1 a new free surface is calculated which, since this is the first time interval, will be a horizontal line. On the horizontal line new mesh points are added to the domain where the vertical lines of the original domain cross the new free surface. The domain at this time will in general look like Figure 6. The velocity potential on the new free surface is calculated for use as a boundary condition. After this is completed, successive over-relaxation calculations are again carried out on the new extended domain.

After these calculations have converged sufficiently, another time increment is computed to advance from t_1 to t_2. Added free surface mesh points and the velocity potential on the new free surface are calculated, followed by another round of successive over-relaxation calculations. This general procedure is carried out until the time of interest or the wetted semi-width of interest is reached.

B. Description of Initial Domain

Initially, the domain for solution is rectangular. To improve the accuracy in the region nearest the keel, the domain is subdivided into a very fine mesh throughout the upper left part of the domain. A less fine mesh is used over an outer subregion in the upper left area of the domain. The balance of the domain is subdivided with a relatively coarse mesh. Let h represent the mesh size of the finest mesh; then the intermediate mesh size is 2h and the coarse mesh size is 4h.

The transition from the finest mesh to the intermediate mesh and the transition from the intermediate mesh to the coarse mesh are done in the same manner as [5]. The programming problems encountered in computing over a domain subdivided in this manner were overcome through the use of a series of computed GO TO statements in FORTRAN which were used to make the appropriate transfers for proper computation of subscript values. The values of ϕ' at the mesh points of the original domain are stored in an array sequentially from left to right, top to bottom.

Actually, of course, equation (11b) is not used in the form shown. It is rewritten as a successive over-relaxation equation in the form (c.f. equation (26))

$$\phi'^{(n+1)} = \frac{\omega}{4}\left(\phi_1'^{(n)} + \phi_2'^{(n+1)} + \phi_3'^{(n+1)} + \phi_4'^{(n)}\right) - (\omega - 1)\,\phi_0'^{(n)} \tag{36}$$

Computations on the line of symmetry (the left-hand boundary of the domain shown in Figure 5) are based on equation (16). However, the program uses equation (36), computing subscripts so that ϕ_1' is used instead of ϕ_3' in equation (36).

Points on the lower boundary of the domain represent the boundary conditions at infinity and consequently the value of ϕ' is identically zero on this boundary, as well as on the right-hand boundary.

Referring to Figure 5, a few examples of the subscripts which would be calculated and used by the program in equation (36) are given.

$$\phi_{19}'^{(n+1)} = \frac{\omega}{4}\left(\phi_{20}'^{(n)} + \phi_2'^{(n+1)} + \phi_{18}'^{(n+1)} + \phi_{29}'^{(n)}\right) - (\omega - 1)\,\phi_{19}'^{(n)} \tag{37a}$$

$$\phi_{133}'^{(n+1)} = \frac{\omega}{4}\left(\phi_{116}'^{(n+1)} + \phi_{118}'^{(n+1)} + \phi_{142}'^{(n)} + \phi_{143}'^{(n)}\right) - (\omega - 1)\,\phi_{133}'^{(n)} \tag{37b}$$

$$\phi_{165}'^{(n+1)} = \frac{\omega}{4}\left(\phi_{166}'^{(n)} + \phi_{142}'^{(n+1)} + \phi_{163}'^{(n+1)} + \phi_{178}'^{(n)}\right) - (\omega - 1)\,\phi_{165}'^{(n)} \tag{37c}$$

$$\phi'^{(n+1)}_{147} = \frac{\omega}{4}\left(\phi'^{(n)}_{148} + \phi'^{(n+1)}_{134} + \phi'^{(n)}_{148} + \phi'^{(n)}_{157}\right) - (\omega - 1)\,\phi'^{(n)}_{147} \tag{37d}$$

Initially all of the values of ϕ' at the points in the original domain (e. g., Figure 5) are set to zero. It should also be noted that the configuration of points shown in Figure 5 is the minimum configuration which the program will handle.

C. Description of Mesh

The mesh size of the finest mesh and the extent of the domain and the extent of the subregions are specified as input parameters, the only restriction being that the extents mentioned above must be multiples of the mesh size. The fine mesh and the intermediate mesh will automatically be square subregions. The complete domain may be rectangular if desired.

D. Progression to Next Time

In computing the time increments, a trial and error procedure is used. The procedure consists of considering each of the points on the hull whose half widths are multiples of h. The time required for each point to become wet is computed using the equation

$$\Delta t = \frac{Y_b(x) - Y_p(x)}{v - u\,\frac{Y(x+h) - Y(x-h)}{2h}} \tag{38}$$

where $Y_b(x)$ is the height of the hull point above the original free surface, the $Y_s(x)$ are points on the free surface, and u and v are found by equations (6c) and (6d). This equation is derived from equation (21). Each of these time increments is compared against an input parameter which specifies the assigned time increment desired. The computed time which is closest to the time increment desired is selected for proceeding to the next step of the computations.

The point on the hull corresponding to this time increment becomes the new contact point. For each mesh interval to the right of this new contact point, the new free surface is computed using equation (21). If this is the first forward step in time, this new free surface will be a horizontal line. For any succeeding time increment, the free surface will in general be a decreasing function from the contact point to the right boundary. The velocity potential on the new free surface, which will be used as new boundary conditions, is computed according to equations (23) and (24). Here again the first step yields a special case; namely, that the velocity potential on the new free surface is identically zero.

All mesh points added by the processes outlined above are placed sequentially in another array in the program. An example of the general numbering scheme is shown in Figures 6 and 7.

It will be noted that in equation (38) it is necessary to determine the vertical distance of the hull-point under consideration above the original free surface of the water. This is done by a subroutine, FORM, which computes the corresponding vertical distances and also the cosines of the angles which the normal to the hull makes with the x and y axes at that point. To use the main FORTRAN program for any convex hull configuration, it would be necessary only to write a short and simple FORM routine for each shape desired. In the current work, subroutines have been prepared for both the circular cylinder and the Mariner section.

E. Special Equations in the Initial Domain

Referring to Figure 6, there are several points of the original mesh which require special equations. The point on the second row of the original mesh which lies directly under the keel (point 26) requires equation (17), which is used in the form

$$\phi_o'^{(n+1)} = \frac{\omega}{3}\left(2\phi_1'^{(n)} + \phi_4'^{(n)} - Vh\right) - (\omega-1)\phi_o'^{(n)} \tag{39}$$

After each iteration, the value of the boundary condition at the keel (point 1 of the original domain) is calculated using equation (15).

Points 2 through 5 on Figure 6, which are adjacent to one hull point, are computed by an equation of the same general form as equation (11a); this is given in over-relaxation form by:

$$\phi_o'^{(n+1)} = \frac{c}{s_o}\left(s_1\phi_1'^{(n)} + s_3\phi_3'^{(n+1)} + s_4\phi_4'^{(n)} + s_c\right) - (\omega-1)\phi_o'^{(n)} \tag{40a}$$

where,

$$C = \frac{\omega}{(h + k_2)} \tag{40b}$$

$$S_0 = 1 - \frac{h^2}{(h+k_2)} \left[\left(\frac{k_2 \cos(n,x)}{h \cos(n,y)} \right) + 1 \right] \tag{40c}$$

$$S_1 = \frac{k_2}{2} - \left(\frac{k_2 \cos(n,x)}{h \cos(n,y)} \right) \left(\frac{h^2}{(h+k_2)} \right) \tag{40d}$$

$$S_3 = \frac{k_2}{2} \tag{40e}$$

$$S_4 = \frac{h k_2}{(h+k_2)} \tag{40f}$$

$$S_c = - \frac{V k_2 h^2}{(k_2 + h)} \tag{40g}$$

where interpolation of the value of the velocity potential on the hull has been done as in [5] and $h = k_1 = -h_3 = -k_4$. This can also be obtained by equations (13a), (13b), (14) and equation (11a) without interpolation.

Points on the first row of the original domain (points 5 through 24 in Figure 6) likewise use an equation of the form of equation (11a) and given in over-relaxation form by

$$\phi_o'^{(n+1)} = \frac{\omega}{(h+k_2)} \left[\frac{k_2 \phi_1'}{2} + \frac{h^2 \phi_2'}{(h+k_2)} + \frac{k_2 \phi_3'}{2} + \frac{h k_2 \phi_4'}{(h+k_2)} \right] - (\omega - 1) \phi_o'^{(n)} \tag{41}$$

where (11a) has been simplified by the fact that $h = k_1 = -h_3 = -k_4$ for these points.

F. Relaxation Equations in the Added Domain

For points which lie on the first row of the added domain three different equations are used. The value of ϕ' at the first point on the first added row which is not a hull point (e. g., point 5 of Figure 7) is found from an equation derived by substituting equation (14) into equation (18) twice to interpolate out points 2 and 3. Written in over-relaxation form, this is:

$$\phi_o'^{(n+1)} = \frac{C}{S_o}\left(S_1\phi_1'^{(n)} + S_4\phi_4'^{(n)} + S_5\phi_5'^{(n)} + S_c\right) - (\omega - 1)\,\phi_o'^{(n)} \tag{42a}$$

where

$$S_o = 1 + \frac{k_4\left[2k_{53}(k_1k_4 + h^2) + k_{135}\right]\left[(k_2 - k_1)\cos_2(n,x) + h\cos_2(n,y)\right]}{d_2} \tag{42b}$$

$$S_1 = -k_2k_4k_{24}k_{53} + \frac{k_4\left\{2k_{53}\left[k_1k_4 + h^2\right] + k_{135}\right\}k_2\cos_2(n,x)}{d_2} \tag{42c}$$

$$S_4 = k_2k_4k_{24}\left\{\frac{k_{15}k_{53}\cos_3(n,x)}{d_1}\right\} + k_2\left[2k_{53}\left\{k_1k_2 + h^2\right\} + k_{135}\right] \tag{42d}$$

$$S_5 = k_2k_4k_{24}\left\{k_{31} + \frac{k_{15}\left[h\cos_3(n,y) - (k_4 - k_3)\cos_3(n,x)\right]}{d_2}\right\} \tag{42e}$$

$$S_c = \frac{k_2k_4k_{24}k_{15}hk_{53}V\cos_3(n,y)}{d_1} + \frac{\left[k_4\left\{2k_{53}\left[k_1k_4 + h^2\right] + k_{135}\right\}\right]\left[hk_2V\cos_2(n,y)\right]}{d_2} \tag{42f}$$

$$C = \frac{\omega}{2k_{24}\left[k_{23}\left(k_1\{k_4+k_2\}-h^2-k_2k_4\right)+k_{135}\right]} \tag{42g}$$

$$d_1 = (k_3-k_4)\cos_3(n,x) + h\cos_3(n,y) \tag{42h}$$

$$d_2 = -k_1\cos_2(n,x) + h\cos_2(n,y) \tag{42i}$$

$$k_{ij} = k_i - k_j \tag{42j}$$

$$k_{135} = -k_1^2k_{23} + k_3^2k_{15} + k_5^2k_{31} \tag{42k}$$

and $\cos_i(n, x)$ is the cosine between the normal to the hull and the x-axis at the i'th point.

On the first added row, if a point is adjacent to only one hull point, the equation is derived from equation (11a) in a manner similar to the derivation of equations (40), but with $h = h_1 = -h_3$. Examples of such points are points 6 and 7 on Figure 7 and the equations are

$$\phi_o'^{(n+1)} = \frac{C}{S_o}\left(S_1\phi_1'^{(n)} + S_3\phi_3'^{(n+1)} + S_4\phi_4'^{(n)} + S_c\right) - (\omega-1)\phi_o'^{(n)} \tag{43a}$$

where

$$C = \frac{\omega k_4}{(k_2k_4 - h^2)} \tag{43b}$$

$$S_o = 1 - \left(\frac{h^2}{(k_2 - k_4)}\right)\left(\frac{k_2 \cos(n,x)}{h \cos(n,y)} + 1\right) \tag{43c}$$

$$S_1 = \frac{k_2}{2} - \left(\frac{k_2 \cos(n,x)}{h \cos(n,y)}\right)\left(\frac{h^2}{k_2 - k_4}\right) \tag{43d}$$

$$S_3 = \frac{k_2}{2} \tag{43e}$$

$$S_4 = -\frac{k_2 h^2}{k_4 (k_2 - k_4)} \tag{43f}$$

$$S_c = -\frac{V k_2 h^2}{(k_2 - k_4)} \tag{43g}$$

At all other points on the first added row (e. g., points 8 through 24 of Figure 7), the value of Φ' is computed by the equation

$$\phi_o'^{(m+1)} = \frac{\omega}{(k_2 k_4 - h^2)}\left[\frac{k_2 k_4 \phi_1'^{(m)}}{2} + \frac{h^2 k_4 \phi_2'^{(m+1)}}{k_2 - k_4} + \frac{k_2 k_4 \phi_3'^{(m+1)}}{2} - \frac{h^2 k_2 \phi_4'^{(m)}}{(k_2 - k_4)}\right] - (\omega - 1)\phi_o'^{(m)} \tag{44}$$

This is derived from equation (11a) using $h = h_1 = -h_3$ and then writing in over-relaxation form.

For points on the second and all succeeding rows, there are also three cases to distinguish. First, points adjacent to two hull points will use equations (42). An example of this case is point 28 on Figure 7.

Second, values of Φ' at points with one adjacent point on the hull (e. g., points 29 and 30 on Figure 7) are calculated by an equation based on equation (19):

$$\phi_o'^{(m+1)} = \frac{C}{S_o}\left(S_1\phi_1'^{(m)} + S_3\phi_3'^{(m+1)} + S_4\phi_4'^{(m)} + S_5\phi_5'^{(m)} + S_c\right) - (\omega - 1)\phi_o'^{(m)} \tag{45a}$$

where

$$C = \frac{\omega}{2k_{24}\left\{k_{53}\left[k_1(k_4+k_2) - h^2 - k_2k_4\right] + \frac{1}{2}k_{135}\right\}} \tag{45b}$$

$$S_o = 1 + \frac{k_4\left\{2k_{53}\left[k_1k_4 + h^2\right] + k_{135}\right\}\left\{(k_2-k_1)\cos(n,x) + h\cos(n,y)\right\}}{d} \tag{45c}$$

$$S_1 = -k_2k_4k_{24}k_{53} + \left[\frac{k_4\left\{2k_{53}\left[k_1k_4+h^2\right] + k_{135}\right\}\left\{k_2\cos(n,x)\right\}}{d}\right] \tag{45d}$$

$$S_3 = k_2k_4k_{24}k_{15} \tag{45e}$$

$$S_4 = k_2\left[2k_{53}\left\{k_1k_2 + h^2\right\} + k_{135}\right] \tag{45f}$$

$$S_5 = k_2k_4k_{24}k_{31} \tag{45g}$$

$$S_c = \frac{k_4\left\{2k_{53}\left[k_1k_4 + h^2\right] + k_{135}\right\}\left\{hk_2V\cos(n,y)\right\}}{d} \tag{45h}$$

$$d = -k_1\cos(n,x) + h\cos(n,y)\,. \tag{45i}$$

The k's are as defined in equations (42).

Third, all other points use an equation based on equation (10a), which when simplified and written in over-relaxation form is

$$\phi_o'^{(n+1)} = C\left(S_1\phi_1'^{(n)} + S_2\phi_2'^{(n+1)} + S_3\phi_3'^{(n+1)} + S_4\phi_4'^{(n)} + S_5\phi_5'^{(n)}\right) - (\omega-1)\phi_o'^{(n)} \tag{46a}$$

where

$$C = \frac{\omega}{2k_{24}\left\{k_{53}\left[k_1(k_4+k_2) - h^2 - k_2k_4\right] + \frac{1}{2}k_{135}\right\}} \tag{46b}$$

$$S_1 = -k_2k_4k_{24}k_{53} \tag{46c}$$

$$S_2 = -k_4\left\{2k_{53}\left[k_1k_4 + h^2\right] + k_{135}\right\} \tag{46d}$$

$$S_3 = k_2k_4k_{24}k_{15} \tag{46e}$$

$$S_4 = k_2\left[2k_{53}\left\{k_1k_2 + h^2\right\} + k_{135}\right] \tag{46f}$$

$$S_5 = k_2k_4k_{24}k_{31}. \tag{46g}$$

The k's are as defined in equations (42).

G. Convergence

At each time step, the criterion for convergence is given by

$$\left|\phi_o'^{(n+1)} - \phi_o'^{(n)}\right| < \delta \tag{47}$$

at all mesh points. At every tenth iteration all mesh points are examined to see if the value of the velocity potential satisfies the convergence criterion, equation (47). An attempt has also been made to establish and include in the computer program a means to detect divergence. However, this method has been found to be applicable only to the first time step. As has been pointed out previously, it is possible to use a value of ω for the over-relaxation factor which is so large that divergence occurs. It was planned that the program would compute its own over-relaxation factor and if such over-relaxation factor were found to cause divergence,* calculations would restart using an over-relaxation factor of one, or alternatively a table of ω's would be stored and they would be used in decreasing order should divergence occur.

H. Calculation of Pressure

After convergence has been achieved for a given time step, the velocity potential at all points on the hull is calculated using equation (14). The pressure on the body is then calculated by the forward difference form of equation (5).

$$p = p_\infty - \rho\left[\frac{\phi'(x,y,t+\delta t) - \phi'(x,y,t)}{\delta t} + \frac{1}{2}\left((v')^2 + 2v'V\right)_{(x,y,t)} + \frac{1}{2}(u')^2_{(x,y,t)} + g(y - Vt)\right] \tag{48}$$

and printout of these values is made.

---

* e.g., the maximum residue grows.

I. Summary

Figure 8 is a simplified flow diagram of the IBM 7090 FORTRAN program which has been written and partially debugged. All parts of the program utilized in making the calculations for the first time step have been thoroughly tested and have produced the results outlined elsewhere in this report. The mechanisms for adding the second, third, and all successive rows of points have not been completely debugged. Likewise, the relaxation computations for the second and all succeeding time steps have not been thoroughly tested.

Nonetheless, the programming approach has adequately demonstrated its generality and flexibility in the computations which have been made for the first time increment for a variety of mesh sizes, mesh extents, over-relaxation factors, and hull shapes.

VIII. DISCUSSION

A. Drawbacks of the Present Method

The present numerical formulation predicts the free surface shape and the free surface boundary values, and then the pressure on the body. If truncation errors and round-off errors both inherent and direct can be reduced to a negligible fraction of the quantities sought, the result would be more accurate theoretically than the simple fitting theory. It would be actually more accurate if the effect of the compressibility and viscosity is really negligible.

The chief drawback of the present numerical scheme (discovered in [2]) is the existence of a singularity at the contact point, at least at the first time step, in the limit of infinitesimal net size. Such singularities are known to occur in incompressible fluid theory when two boundary conditions at one point cannot be fulfilled simultaneously. Nevertheless, the discrepancy with reality in known cases, such as the pressure distribution on an infinitely thin flat plate at an angle of attack, decreases rapidly away from the singularity. Thus the predictions were valuable. The presence of a singularity in the present scheme, however, prevents an accurate description of the free surface shape, which is only approximately constructed by the "piled up" water It is noted that if one elects to stay away from approaching the limiting case of infinitesimal

space net size, there would be no a priori guidance to the accuracy of the solution, while the probable error in pressure in the other limiting case of finite space mesh size with infinitesimal time can be shown to diverge at every point on the body due to finite error in velocity potential. The inability to describe the free surface shape accurately may lead to errors of undesirable magnitude in velocity potential and pressure. For this reason, on one hand, one cannot definitely expect a few per cent error in pressure, even with sufficiently small mesh size. On the other hand, there is a great risk of obtaining erroneous results from insufficiently small space and time mesh sizes. It is possible that the present program may yield an order of magnitude estimate or a result comparable to flat plate fitting theory, but the gain, if any, may not justify the minimum investment required to complete the planned computations for the Mariner section.

The second drawback in the present program is the large demand on machine capacity and computing time, which is, perhaps, inherent with the present numerical formulation. The limitation of machine capacity is a serious obstacle to insuring a sufficiently small space mesh size in the present program. The demand of large computing time on the large computer (IBM 7090) requires a large sum, which is yet unjustified. It seems desirable that the storage requirements(for sufficient accuracy) should be reduced by a factor of about ten or more for further investigation.

B. Future Development

The present numerical formulation is attractive due to its simplicity and is a reasonable preliminary investigation. Future research for a numerical method for ship slamming should remove the drawbacks in the present procedure.

1. Removal of Contact Point Singularity

In order to have a very accurate limiting solution, the implicit contact point singularity should be removed. If not, the free surface shape may not be sufficiently accurate since the spray root is not traced.

(a) Compressibility effect

The velocity in a compressible fluid is always finite, although Mach number can become infinite for expansion around a corner. Therefore, a velocity singularity will not exist at the contact point. Of course, this does not insure accuracy unless the numerical error is negligible.

It is noted that the probable requirement of smaller net size in the spray, when it becomes sharp and curvacious, may be a great hindrance to obtaining a good result at later times (times which may still be quite small). For the initial period with supersonic expansion of semi-wetted width, the method of temporal source can be used, the free surface being flat and the boundary condition on the body being imposed approximately on the unperturbed free surface level. During this period, an analytic solution is more appealing in accuracy and budgeting than a

numerical method. Beyond this period the free surface shape begins to pile up or spray as disturbances are propagated with the local speed of sound. However, the duration in which a computer program yields sufficiently accurate results may be quite short. Another factor is that the barotropic compressible flow equations are more complicated than those for incompressible flow due to the presence of an additional variable, p, the pressure, which has to be solved simultaneously with the other variables. Also, the time step may have to be very small for stability reasons. It is therefore desirable to examine applicability of simplified approaches although there is no a priori assurance of an exceptionally accurate answer.

(b) Iterative scheme

In the conic flow field for two-dimensional water entry [11], the free surface is tangent to the body at all times (> 0), which is quite different from the initial shape in the present method. An iterative scheme was used to determine the free surface shape in [11]. This suggests that the actual free surface shape in an incompressible fluid might be located in such a way that an implicit contact point singularity does not exist. However, a good iterative scheme remains to be developed and examined. Although the number of iterations of any iterative scheme for an accurate free surface shape is yet unknown, one might expect to spend several times more computing time than that for

a similar program for a non-iterative scheme, as in the case if the free surface at each step is reconstructed based on an average velocity during this time step.

2. Reduction of Machine Time

(a) Development of a very fast convergent process for a system of algebraic equations

A recent jump method developed by Doshi* [12] can accelerate the convergence of the successive over-relaxation method perhaps 40% (through private discussions with Dr. Doshi), although investigations have been made on a restricted class of iteration matrices with only real roots and some knowledge of the value of the negative roots. However, due to the irregularity and the growth of the domain in the Euler system and the complexity of the differential equation in the Lagrangian system, an iterative method much faster than the method employed remains to be investigated empirically. However, it cannot reduce considerably—and might even increase—the demand on the memory capacity of a high-speed computer.

(b) Reduction of domain through conformal mapping

For an infinite net, it is possible that the net can be coarser and coarser at larger distances. There is a limit to the number of gradings of the domain in the computer program. Many more branching possibilities must be added for an additional grading.

---

* Senior Research Engineer, Department of Mechanical Sciences, Southwest Research Institute.

Conformal mapping was successful in analytic approaches to many incompressible flow problems by transforming to a desired domain in which simpler solutions can be found. In the present unsteady problem, the interest in the gradient of the potential during a small time interval greatly increased the need of smaller mesh size for higher accuracy. It may be worthwhile to investigate the possibility of reduction in net points after a conformal mapping. The gain, if any, would depend on physical judgment, the complexity of the original domain, and that of the governing differential equations.

(c) Lagrangian coordinates

The irregular nets constructed with each increment of time in the Euler system are not very convenient to program. It is also impractical to find a new transformation to map each new fluid domain into a desired domain, unless a sufficiently large domain is mapped once and for all, in which the boundary contour and free surface at all times of interest are contained. Both of these would become more complex in shape, although the method has the advantage that the Laplacian equation remains the governing equation. Should there be sharp spray in the theory, it is difficult to add fine local nets in the spray at each increment of time in a computer program.

Therefore, it is worthwhile to investigate the use of Lagrangian coordinates which are fixed with the initial domain. There

is some minor difficulty in conformal mapping such as the need of inverse transforms or the calculation of the position in the original domain corresponding to the net constructed in the new domain. But once the derivatives of new coordinates are found, it is valid for all time and independent of the ship section. The over-relaxation method may still be convergent although a rigorous proof might be difficult. Whether there is considerable gain in accuracy and/or computing time in this combined approach remains to be investigated—actual computation may be necessary without sufficient knowledge on the bound of the derivatives of the solution sought. An attempt should also be made to eliminate any implicit singularity, if at all possible.

IX. CONCLUSION

Due to the relatively large funding which would be required to complete the proposed calculations and due to the drawbacks of the method previously discussed, it is concluded that further effort on this program is not warranted. Additional work to develop a new numerical scheme requiring less machine time and predicting pressure distributions and impulses more accurately is required. Certainly, however, the insight and experience gained in the effort reported herein will prove valuable to those developing new approaches and techniques in the future.

REFERENCES

1. Chu, W. H. and Abramson, H. N., "Hydrodynamic Theories of Ship Slamming—Review and Extension", J. Ship Research, Vol. 4, No. 4, Oct. 1961.

2. Chu, W. H., "On the Development of a More Accurate Method for Calculating Body Water Impact Pressures", Tech. Rept. No. 2, Contract No. Nonr. 2729(00), SwRI Project 23-834-2, Sept. 30, 1960.

3. Lamb, H., HYDRODYNAMICS, Sixth edition, Dover Publications, Inc., New York (1945).

4. Milne, W. E., NUMERICAL SOLUTION OF DIFFERENTIAL EQUATIONS, John Wiley & Sons, Inc., New York (1953).

5. Shaw, F. S., AN INTRODUCTION TO RELAXATION METHODS, Dover Publications, Inc., New York, (1953).

6. Young, D. "The Numerical Solution of Elliptic and Parabolic Partial Differential Equations", Space Technology Laboratories, Los Angeles, California, in preparation, May 1958.

7. Young, D. "Iterative Methods for Solving Partial Difference Equations of Elliptic Type", Transactions of the American Mathematical Society, Vol. 76, pp. 92-111, (1954).

8. Forsythe, G. E. and Wasow, W. R., FINITE-DIFFERENCE METHODS FOR PARTIAL DIFFERENTIAL EQUATIONS, John Wiley & Sons, Inc., New York (1960).

9. Taylor, J. L., "Some Hydrodynamic Inertia Coefficients", Philosophical Magazine, Sec. 7, Vol. 9, No. 55, pp. 161-183, Jan. 1930.

10. Schnitzer, E. and Hathaway, M. E., "Estimation of Hydrodynamic Impact Loads and Pressure Distributions on Bodies Approximating Elliptical Cylinders with Special Reference to Water Landings of Helicopters", NACA TN2889, April 1953.

11. Borg, S. F., "Some Contributions to Wedge-Water Entry Problem", Journal of the Engineering Mechanics Division, Proc. ASCE, Vol. 83, No. EM2, April 1957.

12. Doshi, K. D., and Ang, A., "An Accelerated Iterative Procedure for Solving Partial Difference Equations of Elliptic Type", Structure series No. 238, Civil Engineering Studies, U. of Illinois, Urbana, Illinois, (Ph. D. dissertation) April 1962.

APPENDIX A

COMPUTER PROGRAM

Included here is a more detailed flow diagram for the computer program than the one given in Figure 8. The points of the mesh are stored in two different arrays. One array, the PHI-array, contains the points for the original domain; the other array, the P-array contains the points for the added domain.

Table III in Appendix B indicates the transfers necessary to compute properly the subscript values used in calculating the values at the mesh points in the PHI-array. The first column of the table is the line number in the table; the corresponding program variable name is I. The second column is the number of times that this line is to be used in the calculations before proceeding to the next line; the corresponding program variable name is IV. The next five columns are respectively the subscript value for the mesh value being computed followed by the subscript values for the four neighbors being used in the calculation. In each case the subscript value is to be calculated using the formula number shown in the table entry; the corresponding program variable names are I0, I1, I2, I3, I4. The next column indicates the adjustment necessary to the space mesh size as successive points are computed; the corresponding program variable name is DEL. The last column is the number of the equation used for the calculation.

Several other program variable names are used in the formulas of this appendix. These include G1 which is the ordinate (and abscissa) of the extent of the finest mesh, G2 which is the ordinate (and abscissa) of the extent of the intermediate mesh, G3X which is the extent of the complete domain in the horizontal direction, G3Y which is the extent of the complete domain in the vertical direction, and H which is the mesh size for the finest mesh.

Six integers, NUM1, NUM2, NUM3X, NUM3Y, NUMS, and NUMTX are defined by equations A1-A6 following, where XFIXF is the FORTRAN floating to fixed function:

$$NUM1 = XFIXF\ (G1/H + .1) \tag{A1}$$

$$NUM2 = XFIXF((G2 - G1)/(2.0*H) + .1) \tag{A2}$$

$$NUM3X = XFIXF\ ((G3X - G2)/(4.0*H) + .1) \tag{A3}$$

$$NUM3Y = XFIXF\ ((G3Y - G2)/(4.0*H) + .1) \tag{A4}$$

$$NUMS = XFIXF\ (G2/(2.0*H) + .1) \tag{A5}$$

$$NUMTX = XFIXF\ (G3X/(4.0*H) + .1) \tag{A6}$$

Formulas referred to in the table are given following:

$$IV = NUM2-1 \tag{A7}$$

$$IV = NUM1/2-1 \tag{A8}$$

$$IV = NUM3X-1 \tag{A9}$$

$$IV = NUM2 \tag{A10}$$

$$IV = NUMS-2 \tag{A11}$$

$$IV = NUMS/2-1 \tag{A12}$$

```
IV = NUMTX-2                                                    (A13)

IV = 1                                                          (A14)

IV = NUM1/2-2                                                   (A15)

IV = NUM1-1                                                     (A16)

IV = NUMS-1                                                     (A17)

IV = NUMS/2-2                                                   (A18)

IV = NUM2-2                                                     (A19)

IV = NUM3X-2                                                    (A20)

IV = ITAB2(1)-2                                                 (A21)

IV = NUM1 - ITAB2(1) + 1                                        (A22)

I0S = I0S + 2                                                   (A23)

I0 = 1                                                          (A24)

I0 = I0 + 1                                                     (A25)

I0 = I0 + 2                                                     (A26)

I0S = I0 + 1                                                    (A27)

I1 = I0 + 1                                                     (A28)

I1 = I1 + NUM1 + NUM2 + 5                                       (A29)

I1S = I1S + 2                                                   (A30)

I1 = I0 - NUM1 - NUM2 - NUM3X + 1                               (A31)

I1 = I1 + NUM3X + NUMS + 4                                      (A32)

I1 = I0 - NUMS - NUM3X + 1                                      (A33)

I1S = I0S + 1                                                   (A34)

I1 = 2                                                          (A35)
```

```
I1S = I1S + 2                                          (A36)

I1 = I1 + 1                                            (A37)

I1 = I1 + 2                                            (A38)

I1 = I2 + 1                                            (A39)

I2 = I2 + NUM2 + NUM3X + 1                             (A40)

I2 = I2 - NUM1 - NUM2 - NUM3X                          (A41)

I2 = I2 + NUM1 + NUM3X + 1                             (A42)

I2 = I2 + NUM2 + 2                                     (A43)

I2 = I2 - NUM1 - NUM2 - 1                              (A44)

I2 = I2 - NUM2 - NUM3X - 2*NUM1 - 2                    (A45)

I2 = I2 - NUM1                                         (A46)

I2S = I0S - 2 - NUM1                                   (A47)

I2 = I2 + 2                                            (A48)

I2S = I2S + 2                                          (A49)

I2 = I1 - 2                                            (A50)

I2 = I0 - NUMS - 2                                     (A51)

I2 = I0 - NUMS - NUM3X - 1                             (A52)

I2 = I2 - NUMS                                         (A53)

I2S = I0S - NUMS - 2                                   (A54)

DEL = 2.0*DEL                                          (A55)

I2 = I2 - NUM1 + 2                                     (A56)

I2 = I0 - NUM1 - NUM2 - NUM3X - 1                      (A57)

I2 = I2 + 1                                            (A58)
```

```
I2 = I2 - NUMS + 2                                    (A59)

I2 = I0 - NUMTX - 1                                   (A60)

DEL = H                                               (A61)

I2 = I0 - 2*NUMS - NUM3X - 3                          (A62)

I2 = I2 - NUMS - NUM1/2 - NUM3X                       (A63)

I3 = I3 - 1                                           (A64)

I3 = I4                                               (A65)

I3 = I0 + 1                                           (A66)

I3 = I3 - 2                                           (A67)

I3S = I3S + 2                                         (A68)

I3 = I0 + NUM1/2                                      (A69)

I3 = I0 + NUMS/2                                      (A70)

I3S = I0S - 1                                         (A71)

I3 = 0                                                (A72)

I3 = I3 + 1                                           (A73)

I3 = I3 + 2                                           (A74)

I3 = I1                                               (A75)

I4 = I3 + NUM1 + 1                                    (A76)

I4 = I4 + NUM2 + 1                                    (A77)

I4 = I4 - NUM1 - NUM2 - 1                             (A78)

I4 = I4 + NUM2 + NUM3X                                (A79)

I4 = I4 + NUM1/2 + NUM3X + NUM2                       (A80)

I4S = I0S + NUM1 + NUM2 + NUM3X                       (A81)
```

```
I4S = I4S + 1                                    (A82)

I4 = I4 + NUMS + 3                               (A83)

I4 = I3 + 1                                      (A84)

I4 = I0 + NUMS + 2                               (A85)

I4 = I4 + NUM3X                                  (A86)

I4 = NUMS/2 + NUM3X + I4                         (A87)

I4S = I0S + NUMS + NUM3X                         (A88)

I4 = I0 + NUMTX + 1                              (A89)

I4 = I4 + 2                                      (A90)

I4 = NUM1 + NUM2 + NUM3X + 2                     (A91)

I4 = I4 + NUM1 + 3                               (A92)

I4 = I4 + 2*NUM1 + NUM2 + 5                      (A93)

I4 = I4 + 1                                      (A94)

IV = NUM1 - 2                                    (A95)
```

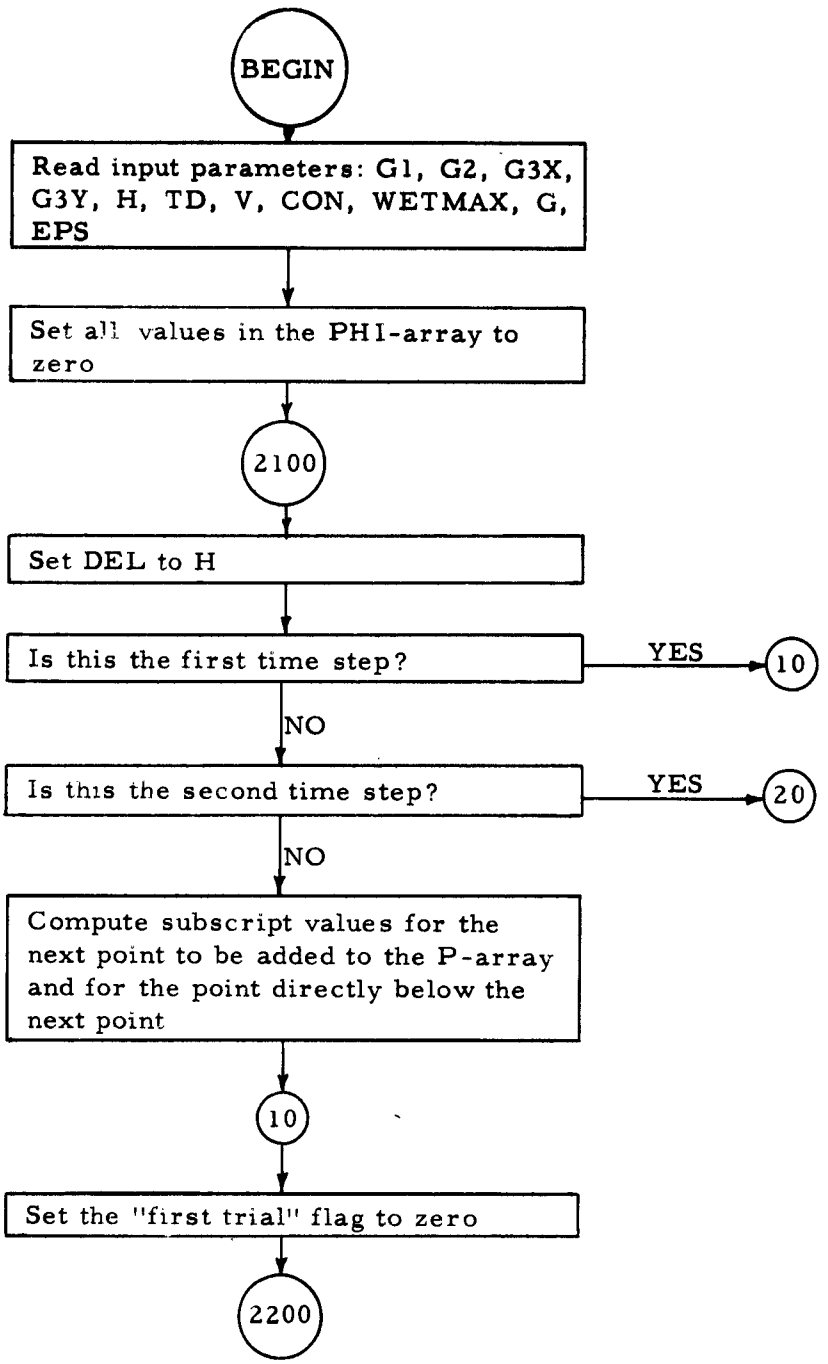
BEGIN
Read input parameters: G1, G2, G3X, G3Y, H, TD, V, CON, WETMAX, G, EPS
Set all values in the PHI-array to zero
2100
Set DEL to H
Is this the first time step?
YES
10
NO
Is this the second time step?
YES
20
NO
Compute subscript values for the next point to be added to the P-array and for the point directly below the next point
10
Set the "first trial" flag to zero
2200

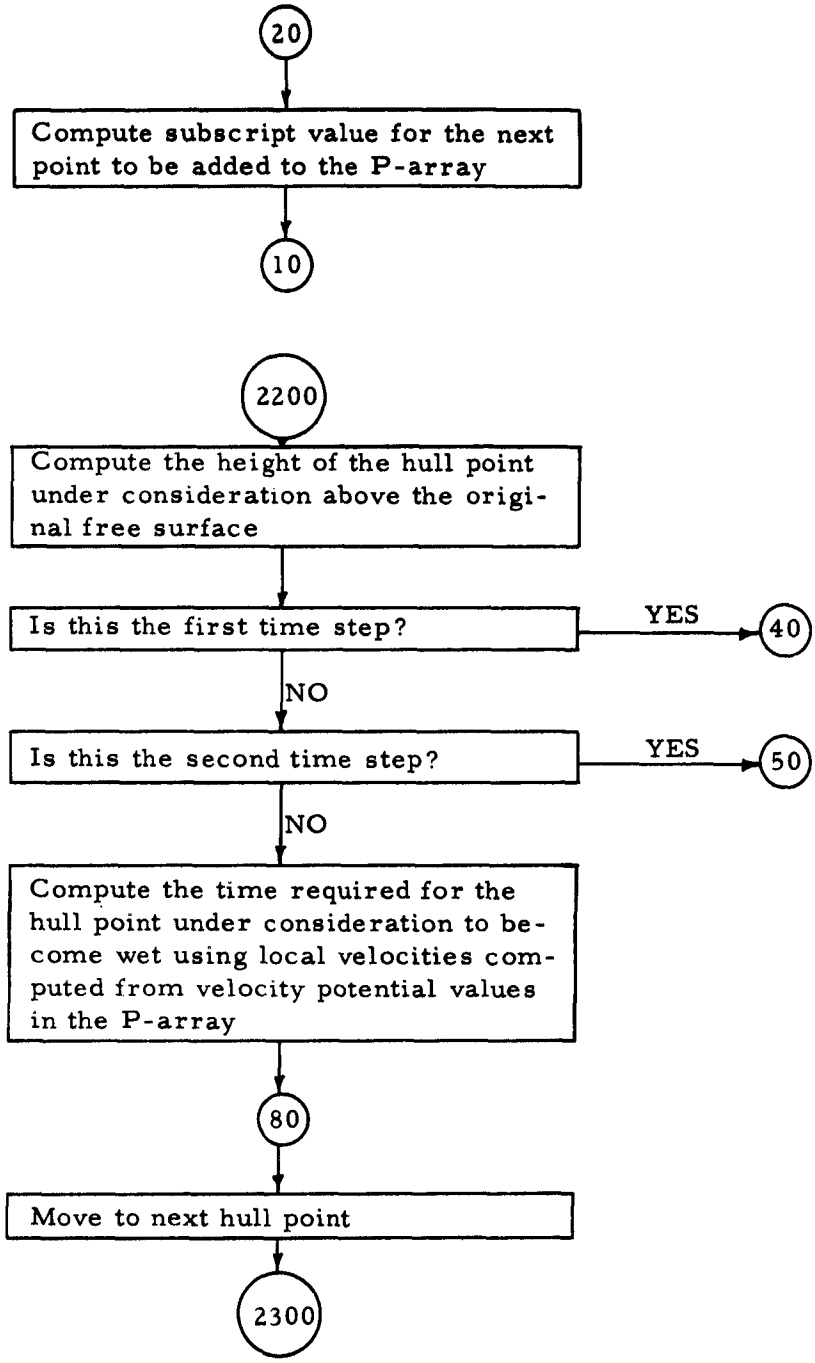
20
Compute subscript value for the next point to be added to the P-array
10
2200
Compute the height of the hull point under consideration above the original free surface
Is this the first time step?
YES
40
NO
Is this the second time step?
YES
50
NO
Compute the time required for the hull point under consideration to become wet using local velocities computed from velocity potential values in the P-array
80
Move to next hull point
2300

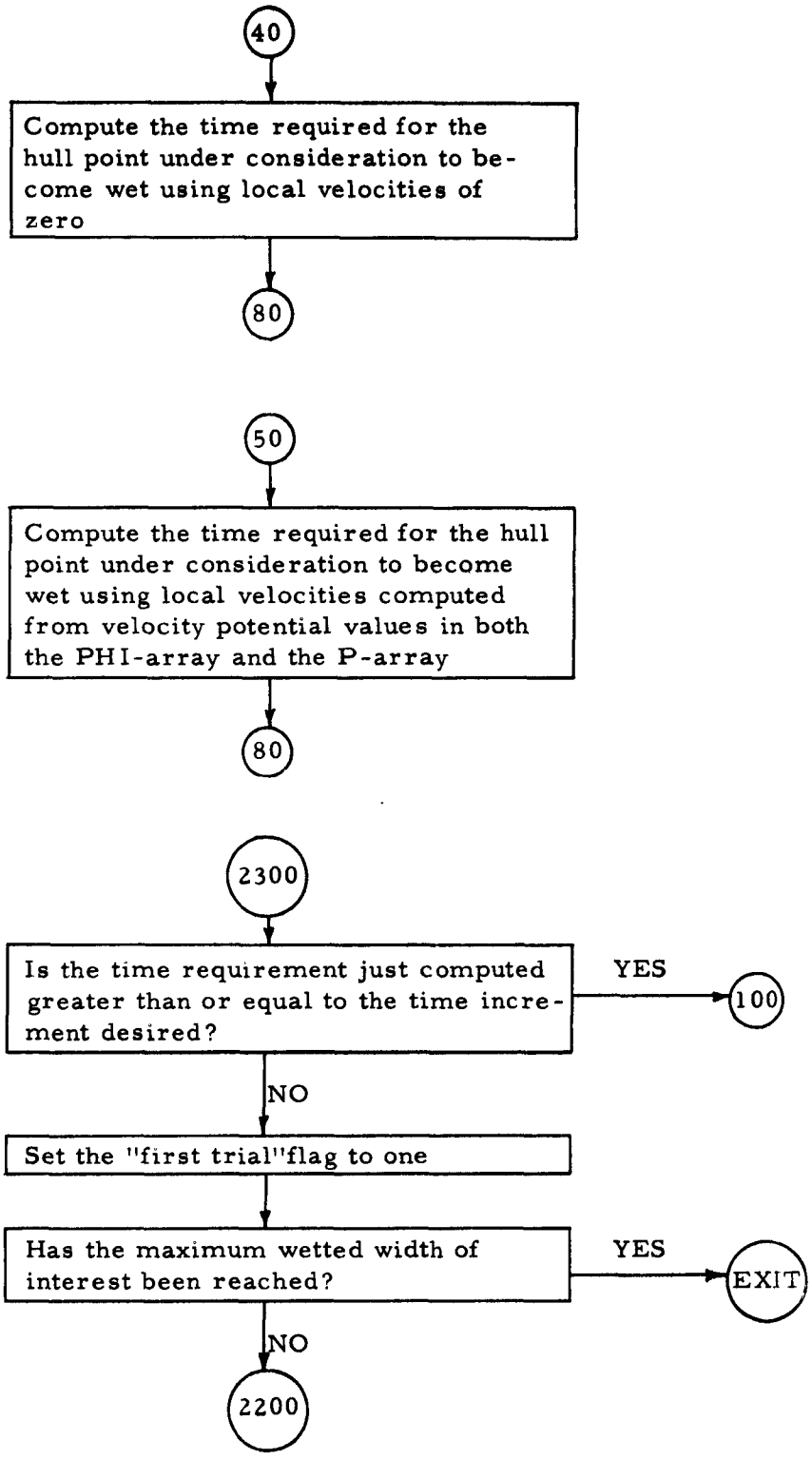
40
Compute the time required for the hull point under consideration to become wet using local velocities of zero
80
50
Compute the time required for the hull point under consideration to become wet using local velocities computed from velocity potential values in both the PHI-array and the P-array
80
2300
Is the time requirement just computed greater than or equal to the time increment desired?
YES
100
NO
Set the "first trial"flag to one
Has the maximum wetted width of interest been reached?
YES
EXIT
NO
2200

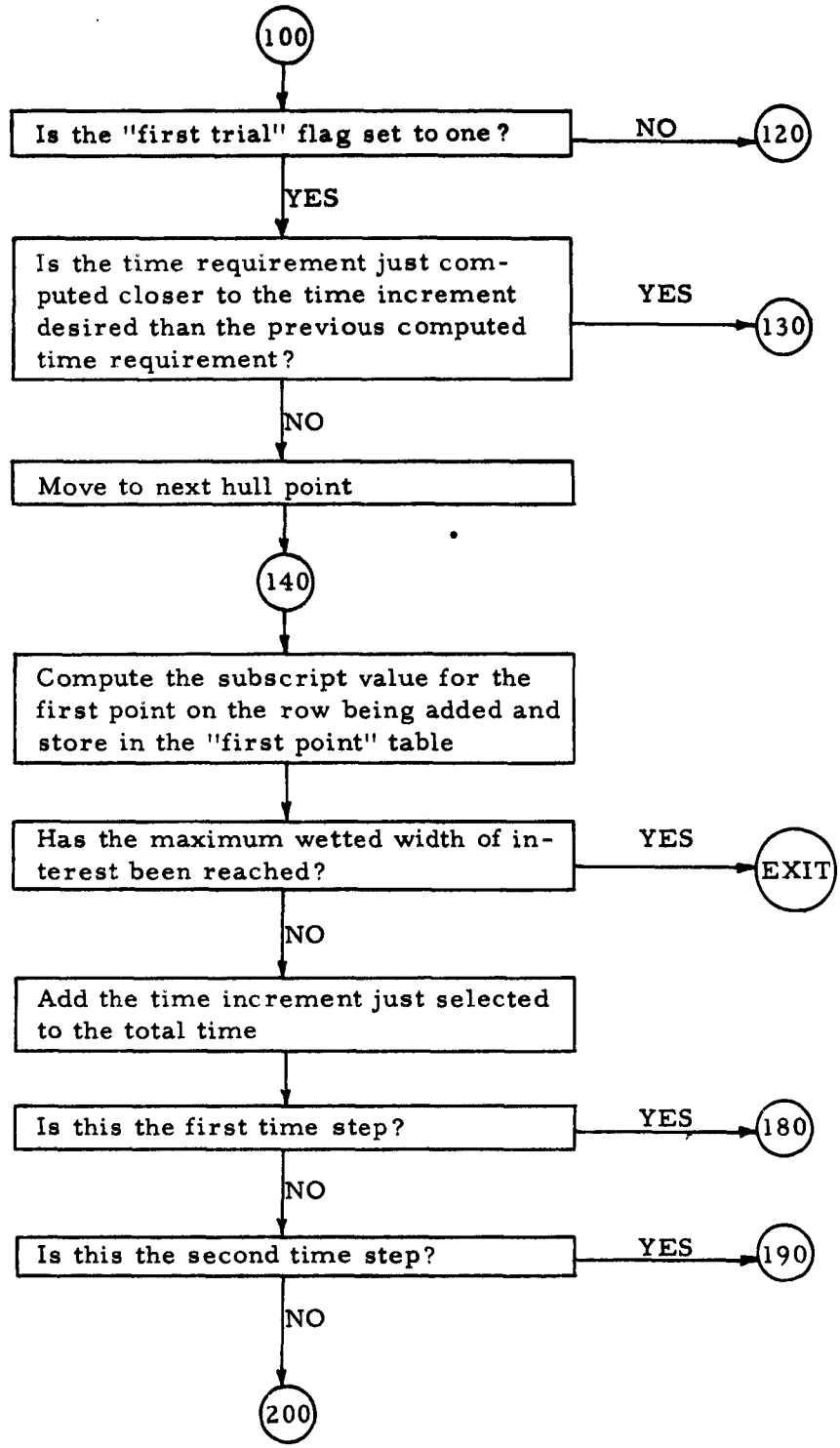
100
Is the "first trial" flag set to one?
NO
120
YES
Is the time requirement just computed closer to the time increment desired than the previous computed time requirement?
YES
130
NO
Move to next hull point
140
Compute the subscript value for the first point on the row being added and store in the "first point" table
Has the maximum wetted width of interest been reached?
YES
EXIT
NO
Add the time increment just selected to the total time
Is this the first time step?
YES
180
NO
Is this the second time step?
YES
190
NO
200

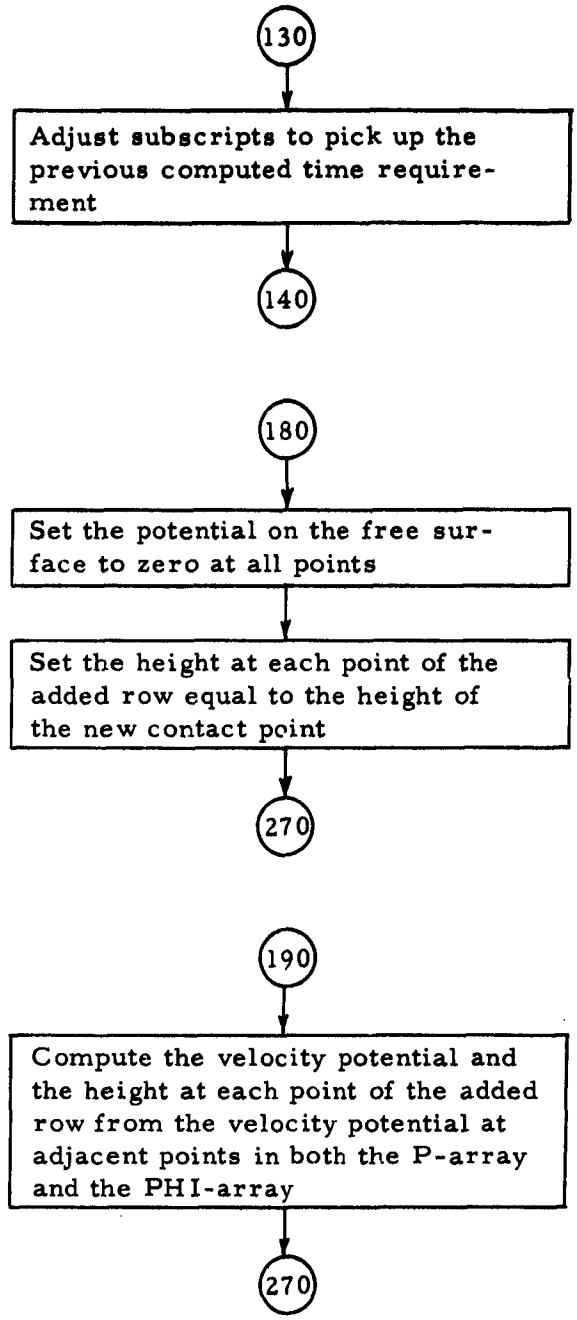
130
Adjust subscripts to pick up the previous computed time requirement
140
180
Set the potential on the free surface to zero at all points
Set the height at each point of the added row equal to the height of the new contact point
270
190
Compute the velocity potential and the height at each point of the added row from the velocity potential at adjacent points in both the P-array and the PHI-array
270

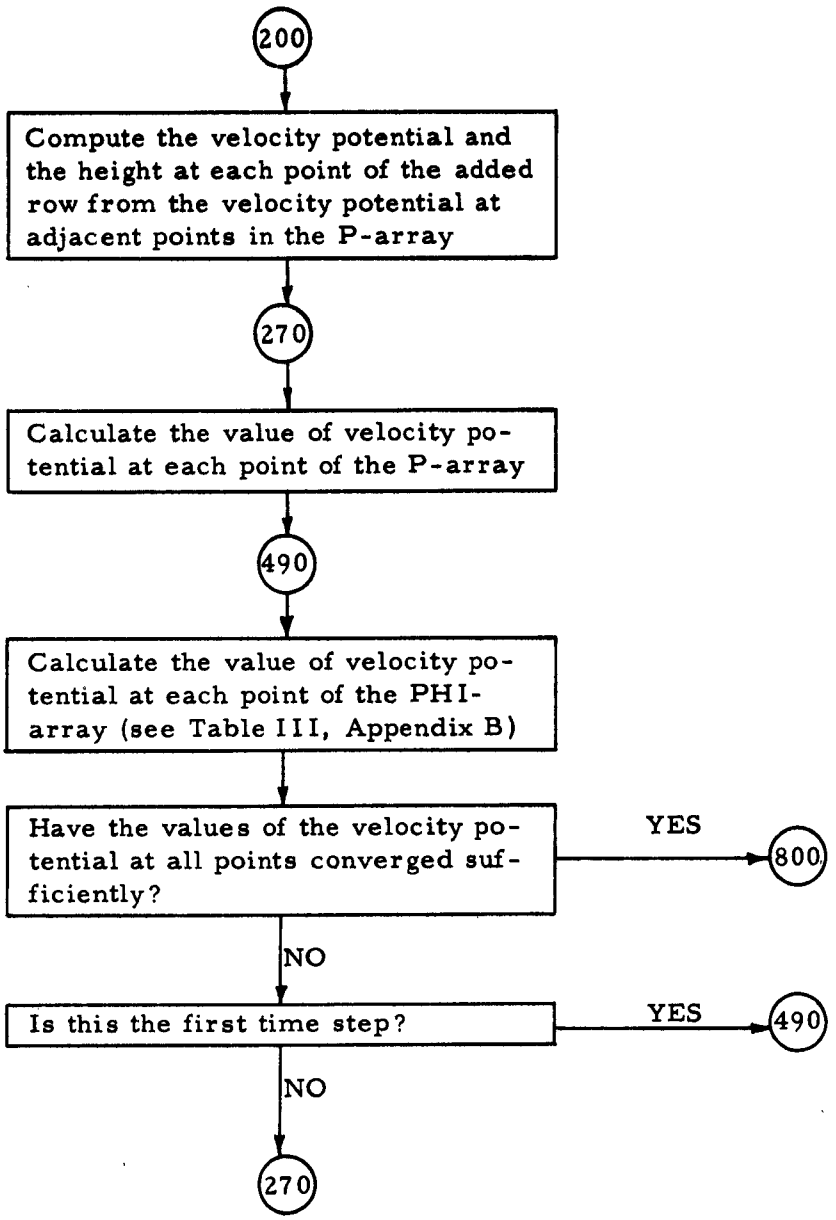
200
Compute the velocity potential and the height at each point of the added row from the velocity potential at adjacent points in the P-array
270
Calculate the value of velocity potential at each point of the P-array
490
Calculate the value of velocity potential at each point of the PHI-array (see Table III, Appendix B)
Have the values of the velocity potential at all points converged sufficiently?
YES
800
NO
Is this the first time step?
YES
490
NO
270

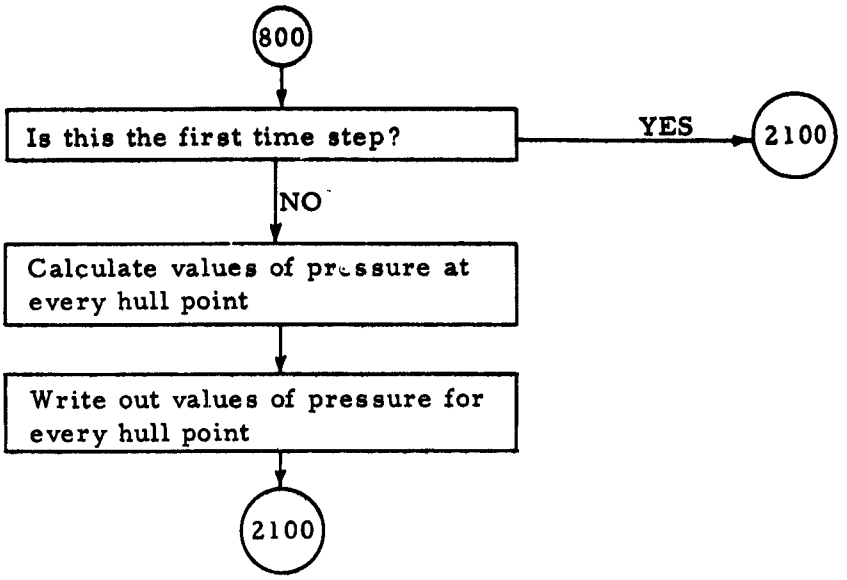
800
Is this the first time step?
YES
2100
NO
Calculate values of pressure at every hull point
Write out values of pressure for every hull point
2100

APPENDIX B

TABLE I: Offsets of Mariner Model (1/20)

y (in.)	x (in.)	y (in.)	x (in.)	y (in.)	x (in.)
0	1.20	0	0	15.00	11.36
0.10	2.30	0.25	3.05	16.00	11.63
0.20	2.87	0.50	3.95	16.20	11.69
0.30	3.31	1.00	5.02	17.00	11.93
0.40	3.66	2.00	6.50	18.00	12.23
0.50	3.95	3.00	7.46	19.00	12.55
0.60	4.21	4.00	8.10	20.00	12.89
0.70	4.45	5.00	8.60	21.00	13.25
0.80	4.68	6.00	9.01	22.00	13.62
0.90	4.87	7.00	9.34	23.00	14.00
1.00	5.02	8.00	9.62	24.00	14.40
		9.00	9.87	25.00	14.82
		10.00	10.12	26.00	15.29
		11.00	10.36	27.00	15.75
		12.00	10.61	28.00	16.25
		13.00	10.85	29.00	16.80
		14.00	11.10	29.70	17.20

y vertical height
x horizontal half-breadth

Gauge Location		Approximate time of contact t_c, sec			Approximate time to end of pressure, t_f sec*		
x	y	(a) V 4.01 fps	(b) V 5.67 fps	(c) V 8.02 fps	(a)	(b)	(c)
0	0	0	0	0	.029	.029	.027
2-1/4"	0.1"	.002,08	.001,47	.001,04	.031	.030	.028
4"	0.51"	.016,2	.007,49	.005,30	.045	.036	.032
6"	1.63"	.033,9	.024,0	.016,93	.064	.053	.044
approximate, b_{mx} (maximum wetted width)		for gauge at 6"			7.51"	7.86"	8.22"
approximate, y_{mx} (depth of submergence)		for gauge at 6"			3.08"	3.62"	4.24"
approximate, b_{mx}		for gauge at 4"			6.66"	6.95"	7.49"
approximate, y_{mx}		for gauge at 4"			2.16"	2.46"	3.08"
approximate, b_{mx}		for gauge at 2-1/4"			5.79"	6.53"	7.19"
approximate, y_{mx}		for gauge at 2-1/4"			1.49"	2.04"	2.69"
approximate, b_{mx}		for gauge at keel			5.67"	6.43"	7.20"
approximate, y_{mx}		for gauge at keel			1.40"	1.97"	2.60"

* Based on estimated time of contact plus the time to end of pressure given by DTMB

TABLE II Time and Width of Interest in Mariner Model Experiments

TABLE III
Transfer Table for Program

I	IV	I0	I1	I2	I3	I4	DEL	Equation
1	A14	A24	A35	----	A72	A91	----	----
2	A21	A25	A37	----	A73	A94	A61	40a
3	A22	A25	A37	----	A73	A94	----	41
4	A14	A25	A37	----	----	A92	A55	41
5	A14	A25	A37	----	A74	A94	----	41
6	A19	A25	A37	----	A73	A94	----	41
7	A14	A25	A37	----	----	A93	A55	41
8	A14	A25	A37	----	A74	A94	----	41
9	A20	A25	A37	----	A73	A94	----	41
10	A14	A26	A38	A57	A75	A76	----	36 or 39
11	A14	A25	A37	A58	A64	A94	----	36
12	A16	A25	A37	A58	A73	A94	----	36
13	A14	A25	A39	----	A65	A94	----	36
14	A14	A25	A28	A40	A66	A77	----	36
15	A14	A25	A37	A58	A64	A94	----	36
16	A95	A25	A37	A58	A73	A94	----	36
17	A14	A25	A37	A41	----	A92	----	36
18	A14	A25	A37	A58	A74	A94	----	36
19	A7	A25	A37	A58	A73	A94	----	36
20	A14	A25	A39	----	A65	A94	----	36
21	A14	A25	A28	A42	A75	A78	----	36
22	A14	A25	A37	A58	A64	A94	----	36
23	A16	A25	A37	A58	A73	A94	----	36
24	A14	A25	A39	----	A65	A94	----	36
25	A14	A25	A28	A43	A75	A79	----	36
26	A14	A25	A37	A58	A64	A94	----	36
27	A95	A25	A37	A58	A73	A94	----	36
28	A14	A25	A37	A44	----	A92	----	36
29	A14	A25	A37	A58	A74	A94	----	36
30	A19	A25	A37	A58	A73	A94	----	36
31	A14	A25	A37	A45	----	A93	----	36
32	A14	A25	A37	A58	A74	A94	----	36
33	A20	A25	A37	A58	A73	A94	----	36
34	A14	A25	A29	A46	A75	A80	----	36
35	A14	A27, A26	A34, A38	A47, A48	A67, A71	A81, A94	----	36
36	A15	A23, A26	A30, A38	A48, A49	A68, A74	A82 A94	----	36
37	A14	A23, A26	A36, A37	A48, A49	A68, A74	A82, A94	----	36
38	A14	A25	A37	A58	A74	A94	----	36
39	A19	A25	A37	A58	A73	A94	----	36

TABLE III (Continued)

I	IV	I0	I1	I2	I3	I4	DEL	Equation
40	A14	A25	A37	A45	----	A83	----	36
41	A14	A25	A37	A58	A74	A94	----	36
42	A20	A25	A37	A58	A73	A94	----	36
43	A14	A26	A31	A50	A69	A84	----	36
44	A8	A25	A38	A48	A73	A94	----	36
45	A14	A25	A28	A56	A75	A85	----	36
46	A14	A25	A37	A48	A64	A94	----	36
47	A8	A25	A37	A48	A73	A94	----	36
48	A10	A25	A37	A58	A73	A94	----	36
49	A14	A25	A39	----	A65	A94	----	36
50	A14	A25	A28	A51	A75	A86	----	36
51	A14	A25	A37	A58	A64	A94	----	36
52	A11	A25	A37	A58	A73	A94	----	36
53	A14	A25	A37	A62 or A63	----	A83	----	36
54	A14	A25	A37	A58	A74	A94	----	36
55	A20	A25	A37	A58	A73	A94	----	36
56	A14	A26	A28	A52	A75	A85	----	36
57	A14	A25	A37	A58	A64	A94	----	36
58	A17	A25	A37	A58	A73	A94	----	36
59	A14	A25	A39	----	A65	A94	----	36
60	A14	A25	A32	A53	A75	A87	----	36
61	A14	A27, A26	A34, A38	A48, A54	A67, A71	A88, A94	----	36
62	A18	A23, A26	A30, A38	A48, A49	A68, A74	A82, A94	----	36
63	A14	A23, A26	A36, A37	A48, A49	A68, A74	A82, A94	----	36
64	A14	A25	A37	A58	A74	A94	----	36
65	A20	A25	A37	A58	A73	A94	----	36
66	A14	A26	A33	A50	A70	A84	----	36
67	A12	A25	A38	A48	A73	A94	----	36
68	A14	A25	A28	A59	A75	A89	----	36
69	A14	A25	A37	A48	A64	A94	----	36
70	A12	A25	A37	A48	A73	A94	----	36
71	A9	A25	A37	A58	A73	A94	----	36
72	A14	A26	A38	A60	A75	A90	----	36
73	A14	A25	A37	A58	A64	A94	----	36
74	A13	A25	A37	A58	A73	A94	----	36
75	A14	A24	----	----	----	A91	----	15

APPENDIX C

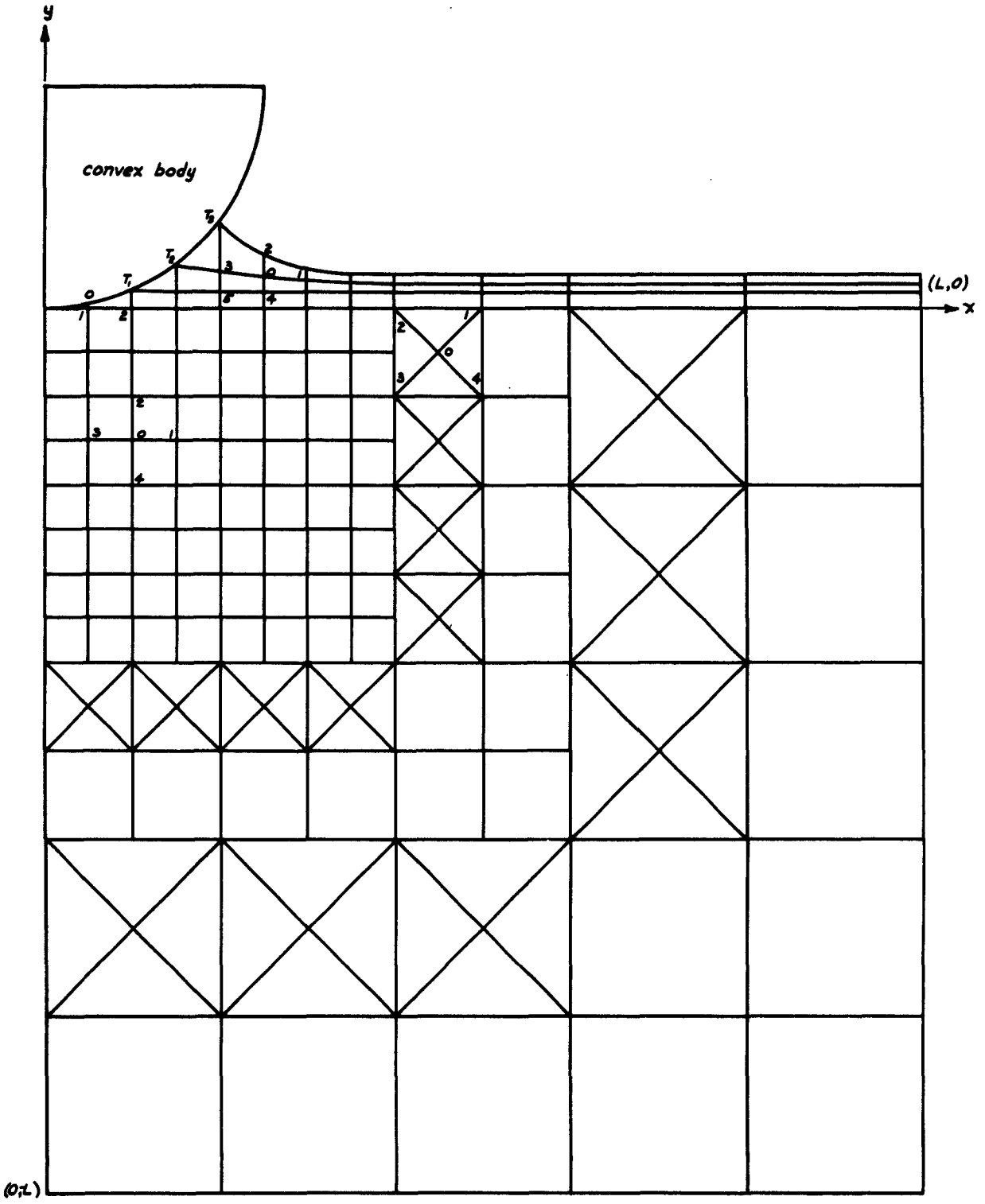

FIGURE 1. SIMPLIFIED NET CONSTRUCTION FOR NUMERICAL PROCEDURE

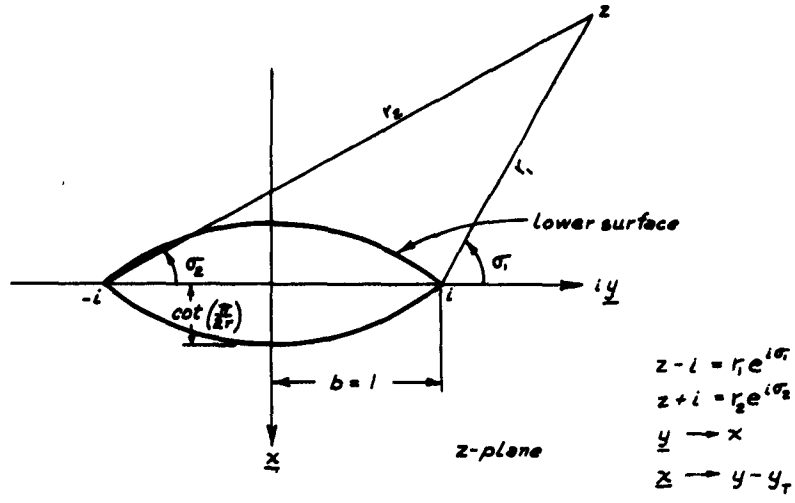

FIGURE 2. COORDINATES FOR FLOW OVER TWO CIRCULAR ARCS

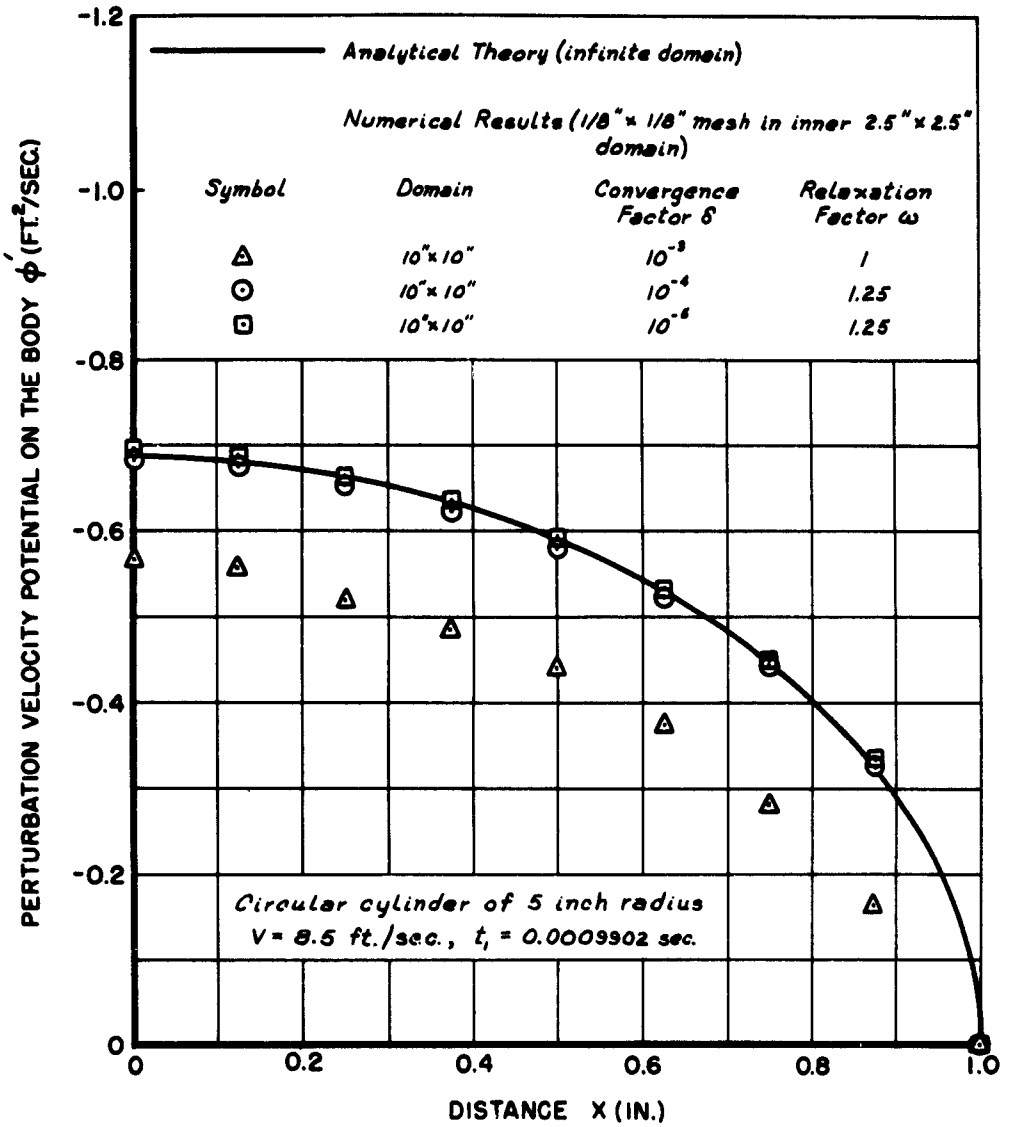

FIGURE 3. COMPARISON OF ANALYTIC THEORY AND NUMERICAL RESULTS AT THE FIRST TIME STEP FOR A CIRCULAR CYLINDER

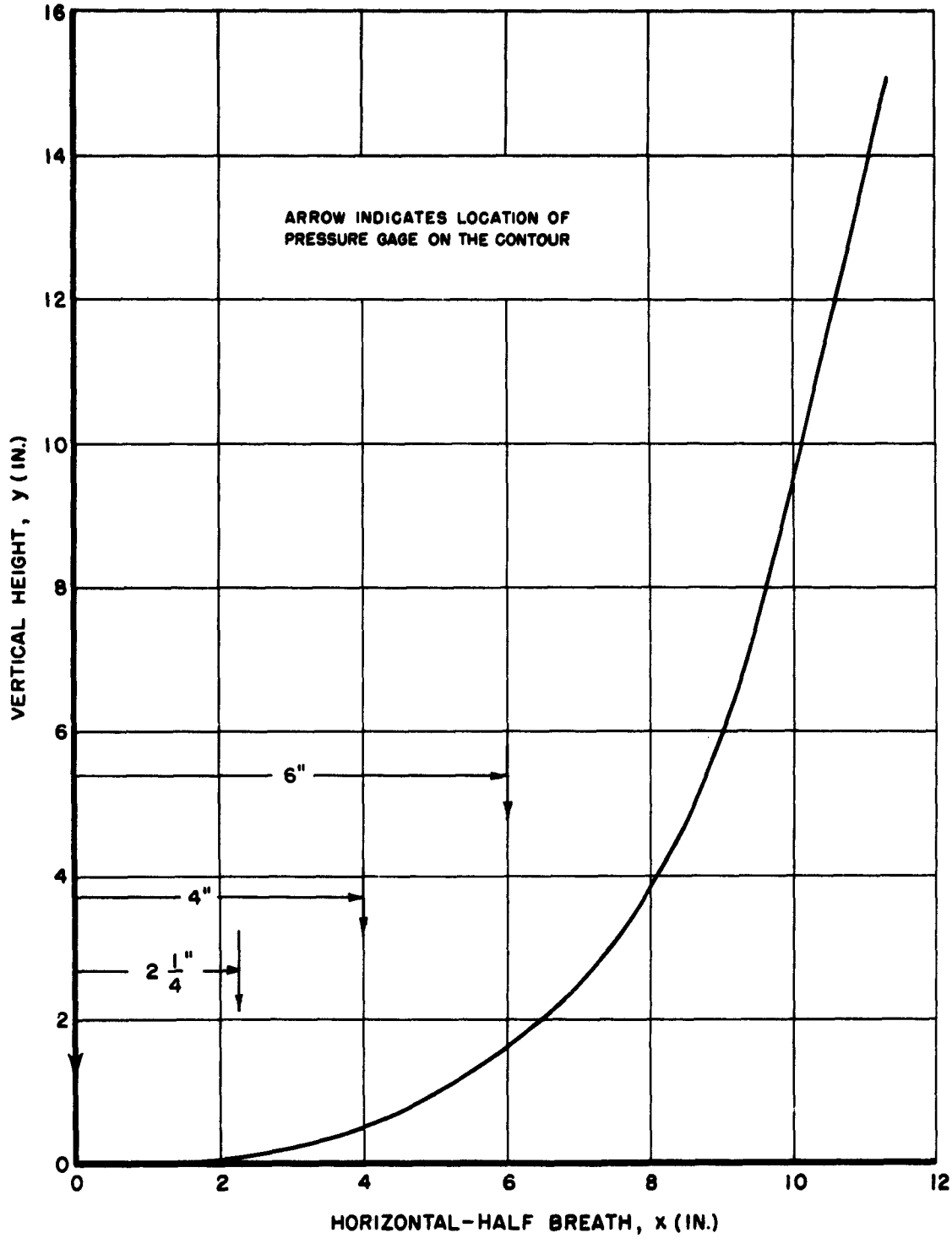

FIGURE 4. MARINER MODEL

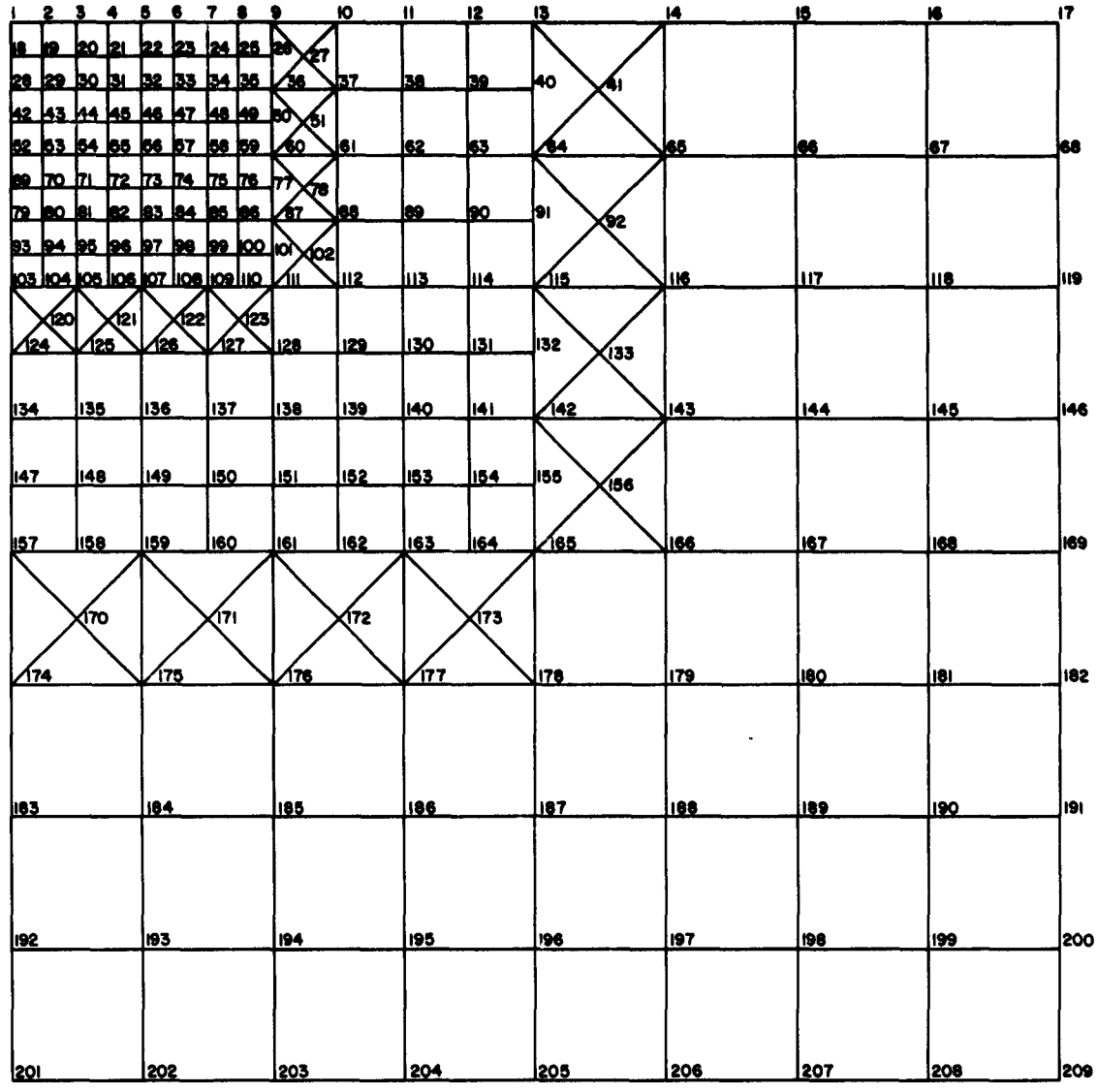

FIGURE 5. MINIMUM MESH CONFIGURATION

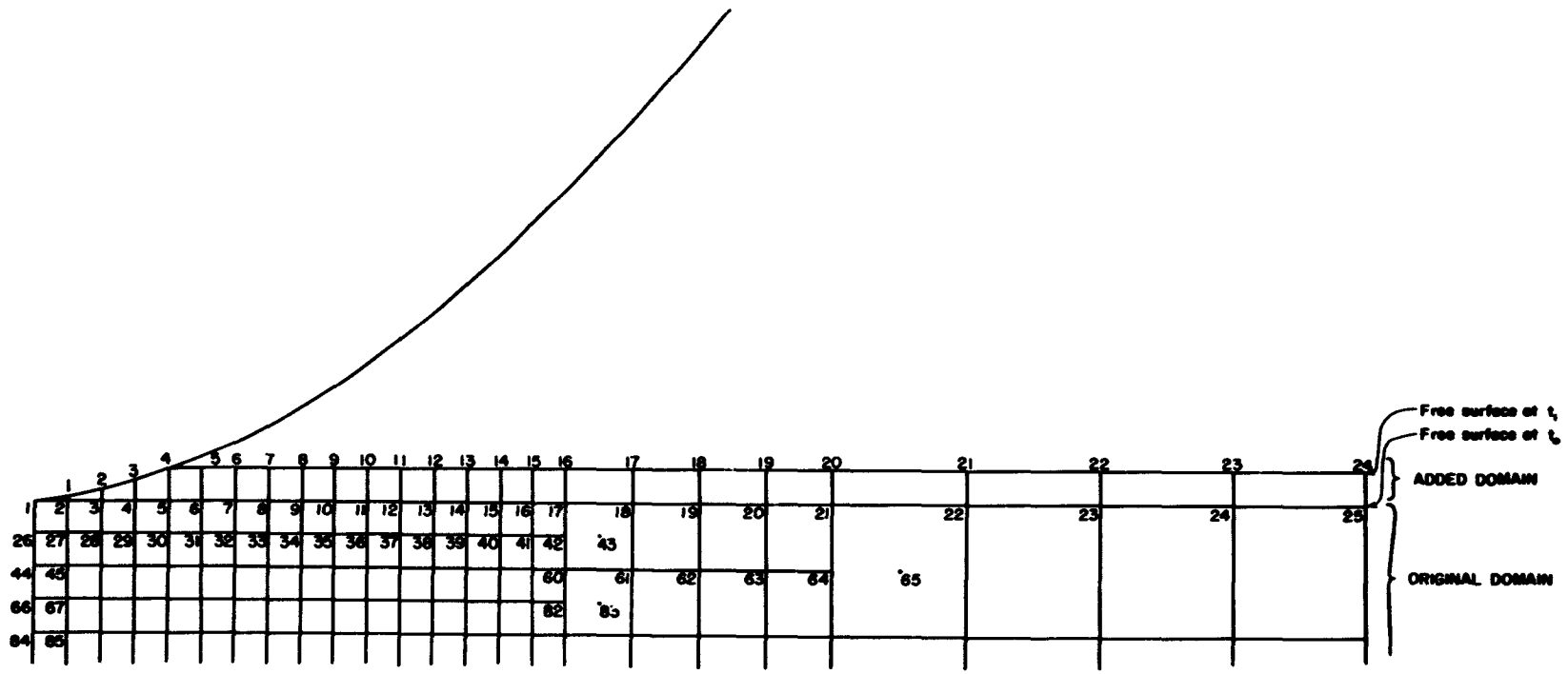

FIGURE 6. TYPICAL DOMAIN WITH FIRST ROW OF POINTS ADDED

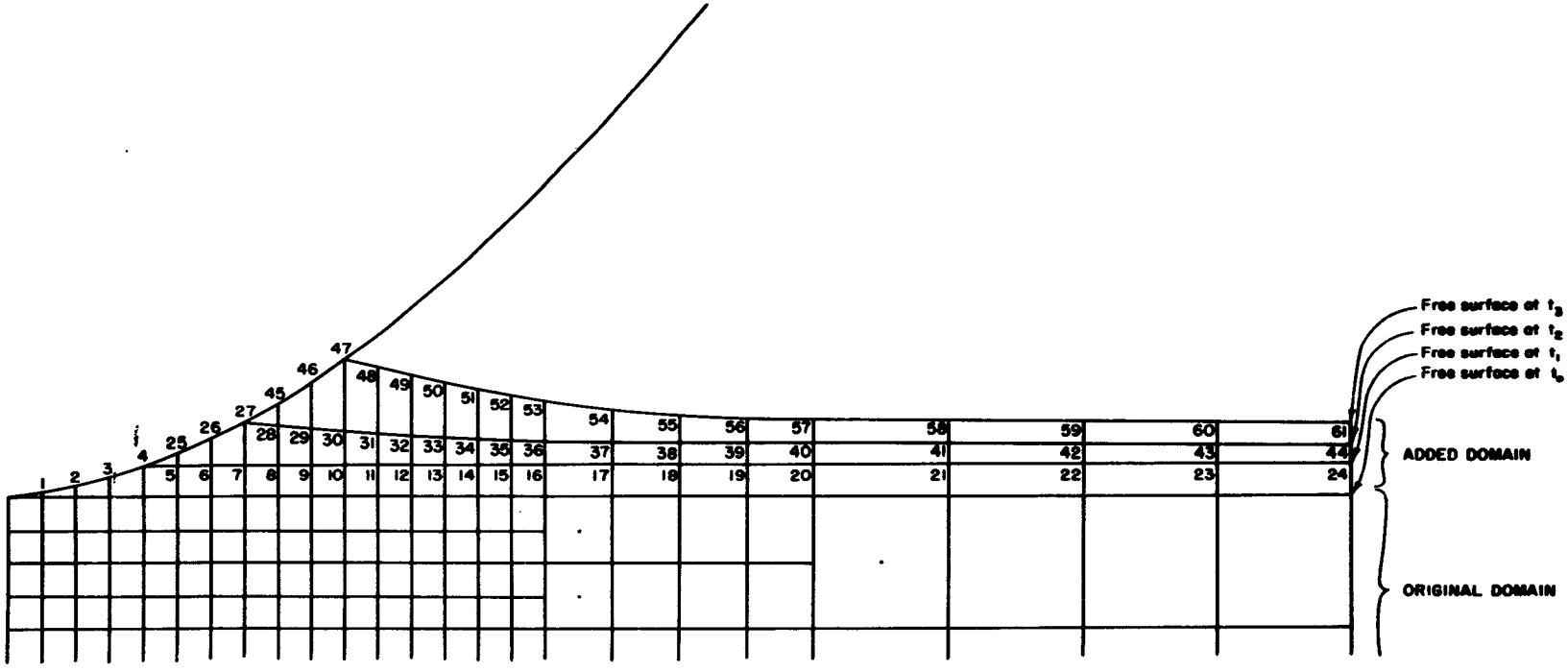

FIGURE 7. TYPICAL DOMAIN WITH THREE ROWS OF POINTS ADDED

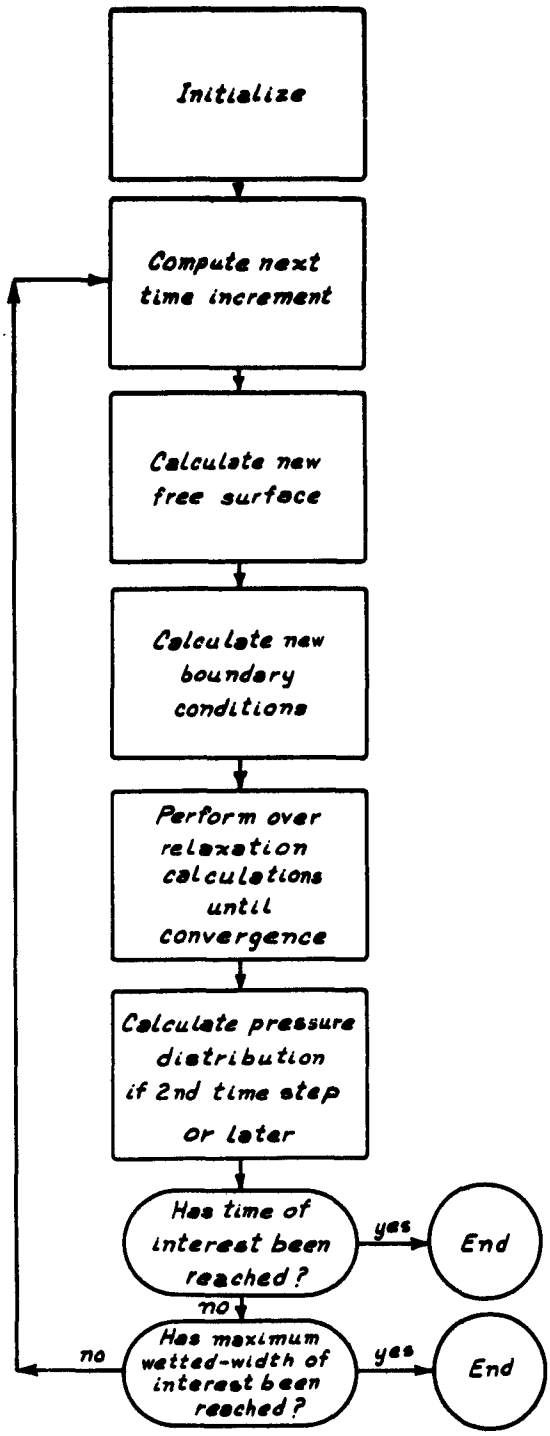

FIGURE 8. SIMPLIFIED FLOW CHART

INITIAL DISTRIBUTION LIST
Contract Nonr-2729(00)

Commanding Officer and Director
David Taylor Model Basin
Washington 7, D. C.
(60) Attn: Code 513

Chief, Bureau of Ships
Department of the Navy
Washington 25, D. C.
(3) Attn: Tech. Info. Section (Code 335)
(1) Applied Science (Code 340)
(1) Ship Design (Code 410)
(2) Prelim. Des. (Code 420)
(1) Hull Design (Code 440)
(1) Noise Reduction (Code 345)
(1) Hull, Arrgts., & Seamanship (Code 341B)
(1) Preliminary Design Section (Code 421)

Chief, Bureau of Weapons
Department of the Navy
(2) Washington 25, D. C.

Chief of Naval Research
Department of the Navy
Washington 25, D. C.
(1) Attn: Fluid Dynamics Branch (Code 438)
(1) Naval Science Division (Code 460)
(1) Undersea Warfare Branch (Code 466)

Commanding Officer
Office of Naval Research
Branch Office
346 Broadway
(1) New York 13, New York

Commanding Officer
Office of Naval Research
Branch Office
Navy No. 100, c/o Fleet Post Office
(1) New York, New York (London, England)

Commanding Officer
Office of Naval Research
Branch Office
1030 E. Green Street
(1) Pasadena, California

Commanding Officer
Office of Naval Research
Branch Office
1000 Geary Street
(1) San Francisco, California

Commanding Officer
Office of Naval Research
Branch Office
John Crerar Library Building
86 E. Randolph Street
(1) Chicago 11, Illinois

Commanding Officer
Office of Naval Research
Branch Office
495 Summer Street
(1) Boston 10, Massachusetts

Commander
Naval Ordnance Laboratory
White Oak
(1) Silver Spring, Maryland

Commander
Naval Ordnance Division
Underwater Ordnance Division
3202 E. Foothill Boulevard
(1) Pasadena 8, California

Commander
Naval Ordnance Division
(1) Inyokern, China Lake, California

Director
U. S. Naval Research Laboratory
(1) Washington 25, D. C.

Office of the Secretary of Defense
Research and Development Division
The Pentagon
(1) Washington 25, D. C.

Director
National Bureau of Standards
(1) Washington 25, D. C.

Chief
Mechanics Branch
Air Research and Development Command
Air Force Office of Scientific Research
14th and Constitution
(1) Washington 25, D. C.

Chief
Dynamics Branch
Aircraft Laboratory
Aeronautical Systems Division
Air Research and Development Command
(1) Wright-Patterson Air Force Base, Ohio

Director
National Aeronautics and Space Administration
1512 H Street, Northwest
(2) Washington 25, D. C.

Director
Langley Research Center
National Aeronautics and Space Administration
(2) Langley Field, Virginia

Commander
ASTIA (TIPDR)
Arlington Hall Station
(10) Arlington 12, Virginia

Guggenheim Aeronautical Laboratory
California Institute of Technology
(1) Pasadena 4, California

Head
Department of Civil Engineering
California Institute of Technology
(1) Pasadena 4, California

Head
Department of Aeronautical Engineering
Massachusetts Institute of Technology
(1) Cambridge 39, Massachusetts

Director
Hydro Laboratory
Department of Civil and Sanitary Engineering
Massachusetts Institute of Technology
(1) Cambridge 39, Massachusetts

Head
Department of Naval Architecture and
Marine Engineering
Massachusetts Institute of Technology
(1) Cambridge 39, Massachusetts

Librarian
Society of Naval Architects and Marine
Engineers
74 Trinity Place
(1) New York 6, New York

INITIAL DISTRIBUTION LIST
Contract Nonr-2729(00)
(Continued)

Editor
Engineering Index, Inc.
29 West 39th Street
(1) New York, New York

Editor
Applied Mechanics Reviews
Southwest Research Institute
8500 Culebra Road
(2) San Antonio 6, Texas

Librarian
American Institute of Aeronautics
and Astronautics
500 Fifth Avenue
(1) New York 36, New York

Director
Ordnance Research Laboratory
Pennsylvania State University
(1) University Park, Pennsylvania

Department of Naval Architecture
University of California
College of Engineering
Berkeley 4, California
(1) Attn: Prof. John V. Wehausen

Applied Mechanics Department
Cornell Aeronautical Laboratory, Inc.
Post Office Box 235
Buffalo 21, New York
(1) Attn: Dr. Irving C. Statler

Illinois Institute of Technology
Technology Center
Chicago 16, Illinois
(1) Attn: Prof. Irving Michelson

Department of Naval Architecture
and Marine Engineering
The University of Michigan
Ann Arbor, Michigan
(1) Attn: Dr. Finn C. Michelsen

Davidson Laboratory
Stevens Institute of Technology
Castle Point Station
Hoboken, New Jersey
(1) Attn: Dr. John P. Breslin
Director

Robert Taggart, Incorporated
400 Arlington Boulevard
Falls Church, Virginia
(1) Attn: Mr. Edgar D. Hoyt

Technical Research Group, Inc.
2 Aerial Way
Syosset, New York
(1) Attn: Dr. Jack Kotik

Vidya
1450 Page Mill Road
Palo Alto, California
(1) Attn: Dr. A. H. Sacks

Oceanics, Incorporated
Technical Industrial Park
Plainview, Long Island, New York
(1) Attn: Dr. P. Kaplan